Fundamentals of Aeroacoustics

Introduction to Aeroacoustics

Aeroacoustics

Discipline that deals with noise generated aerodynamically, multidisciplinary topic, bridging aero and acoustics.

- Difference with acoustics: sound propagation in air with complex situation where sound travels in non uniform flows
- Coupling: Investigates coupling between hydrodynamic (incompressible) and/or entropic (thermal) unsteadiness in a fluid and its acoustic mode. Thermo-acoustic resonance

Flow 0.3 M vs No flow

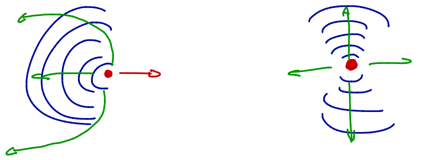

Sound generation: aerodynamics

Sound propagation: aeroacoustics

Phenomenology:

Wind musical instruments: feedback tones through the coupling between unsteady vortical flows in the shear layer, sound waves and acoustic modes.

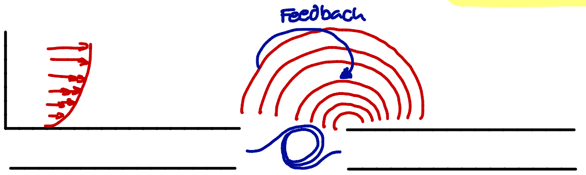

Aircraft Noise:

Jet noise turbulent flow in the engine plume

Fan noise unsteady forces by rotating engine components on surrounding fluid

Airframe noise turbulent flow past the airframe and landing gear

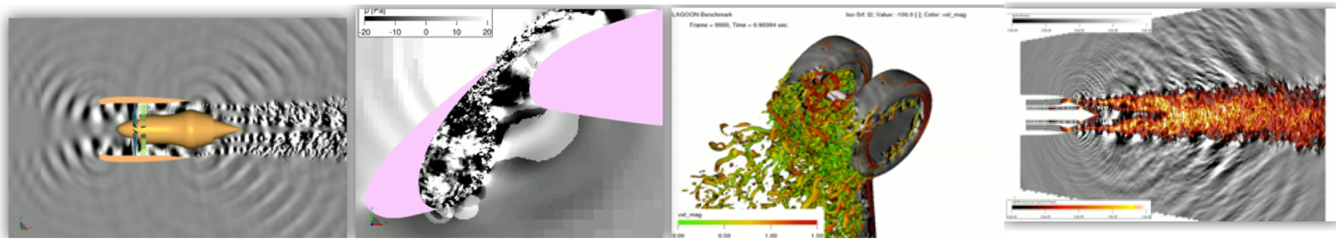

Wind Turbines:

- Noise generated by wall-bounded turbulent fluctuations convected past the trailing edge are responsible for the noise generated. T-E noise! Same for cooling fans

Introduction: (Things to improve & why it changes so much)

- Only a small energy portion generates noise, so two systems with similar performances can produce very different noise levels.
- A lot to do still to reduce noise. Optimize design...
- Aircraft design optimization requires fast and accurate computational predictive methods.
- Active noise control devices needs knowledge

Key Quantities

- Mach number: $M = \frac{v}{c}$
- Reynolds number: $\mathrm{Re} = \frac{\rho v L}{\mu}$
- Reduced frequency (Strouhal number): $\mathrm{St} = \frac{fL}{v}$
- Helmholtz number: $kL = \frac{2\pi f L}{c} \equiv \frac{2\pi L}{\lambda} \equiv 2\pi\,\mathrm{St}\,M$

Helmholtz Number:

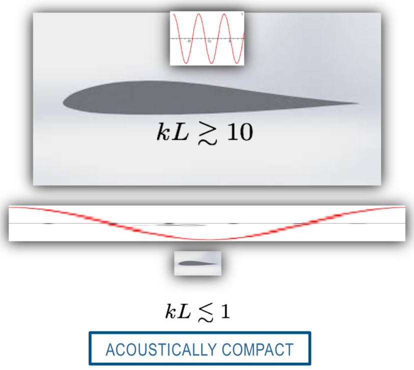

Acoustic Analogy:

Equivalent sources generate the same sound

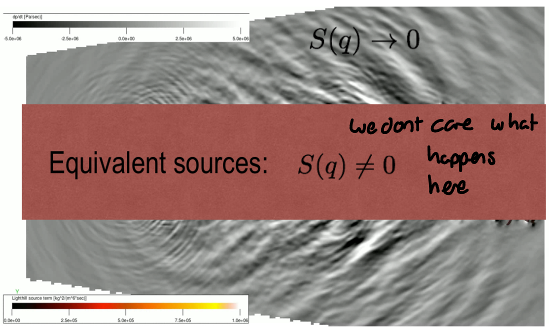

as long as outside is the same.

$$\mathcal{NS}(q) = 0$$

$$\nabla^2 p - \frac{1}{c_\infty^2}\frac{\partial^2 p}{\partial t^2} = S(q)$$

History:

Strouhal: $f_0 = St \cdot \frac{U_0}{d}$ → first related the sound emission to the flow friction, but Lord Rayleigh realized later that actually it was due to periodic vortex shedding.

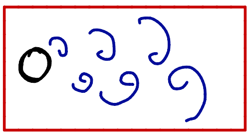

Philips proposed a model of sound generation with 3D, (spanwise)

Sound of flow passing cylinder:

$49 < \mathrm{Re} \lesssim 190$	laminar vortex shedding (2D)
$190 \lesssim \mathrm{Re} < 260$	wake transition (2D/3D)
$260 < \mathrm{Re} \lesssim 1000$	incr. disorder in 3D fine-scale
$1000 < \mathrm{Re} < 200000$	shear-layer transition (3D)

The periodic vortices induce a harmonic lift of tonal frequency f_0 and a drag of frequency of $2f_0$.

CIRCULAR CYLINDER

$$\frac{\partial \rho}{\partial t} + \frac{\partial}{\partial x_i}(\rho u_i) = 0$$ (1) Continuity eq. (mass conservation)

$$\frac{\partial}{\partial t}(\rho u_i) + \frac{\partial}{\partial x_j}(\rho u_i u_j) = -\frac{\partial P}{\partial x_i}$$ (2) linear momentum eq. (Newton's second law) Inviscid $\tau = 0$

? FORCE

$$\frac{\partial (1)}{\partial t} - \frac{\partial (2)}{\partial x_i} \quad \left\{ \begin{array}{l} \frac{\partial^2 \rho}{\partial t^2} + \cancel{\frac{\partial}{\partial x_i}\cdot\frac{\partial}{\partial t}(\rho u_i)} = 0 \\ \cancel{\frac{\partial}{\partial t}\cdot\frac{\partial}{\partial x_i}(\rho u_i)} + \frac{\partial^2}{\partial x_i \partial x_j}(\rho u_i u_j) = -\frac{\partial^2 P}{\partial x_i^2} + \frac{\partial f_i}{\partial x_i} \end{array} \right\} \frac{\partial^2 \rho}{\partial t^2} - \frac{\partial^2}{\partial x_i \partial x_j}(\rho u_i u_j) = \frac{\partial^2 P}{\partial x_i} - \frac{\partial f_i}{\partial x_i}$$

Acoustic fluctuations are so small that can be assumed to be isentropic

$$P = K\rho^{\gamma} \longrightarrow \boxed{\delta p = c_0^2 \, \delta \rho} \longrightarrow c_0 = \sqrt{\frac{\gamma P}{\rho}}$$

Supposing small flow perturbations, low Mach number, quadrople pole can be neglected.

$$\frac{\partial^2 \rho}{\partial t^2} - \cancel{\frac{\partial^2}{\partial x_i \partial x_j}(\rho u_i u_j)} = \frac{\partial^2 P}{\partial x_i} - \frac{\partial f_i}{\partial x_i} \longrightarrow \boxed{\frac{1}{c_0^2}\frac{\partial^2 P}{\partial t^2} - \frac{\partial^2 P}{\partial x_i} = -\frac{\partial f_i}{\partial x_i}}$$

Solution using Green's function.

Green's function:

$$\frac{1}{c_0^2}\cdot\frac{\partial^2}{\partial t^2} G(x,t|y,\tau) - \frac{\partial^2}{\partial x_i^2} G(x,t|y,\tau) = \delta(x-y)\,\delta(t-\tau)$$

$$\boxed{G(x,t|y,\tau) = \frac{\delta\left(t-\tau-\frac{|x-y|}{c_0}\right)}{4\pi|x-y|}} \longrightarrow t-\tau-\frac{|x-y|}{c_0} = 0 \rightarrow \tau = t - \frac{|x-y|}{c_0} \equiv \tau_{ret}$$

Green's formula:

$$P(x,t) = -\int_{-\infty}^{+\infty}\iiint_V G\,\nabla\cdot f\,dy\,d\tau = -\int_{-\infty}^{\infty}\iiint_V \frac{\nabla f(y,\tau)\,\delta\left(t-\tau-\frac{|x-y|}{c_0}\right)}{4\pi|x-y|}\,dy\cdot d\tau$$

Force: suppose the force is concentrated at one point. (x_s)

$$f(y,\tau) = F(\tau)\cdot\delta(y-x_s)$$ Substitude with Diract function

$$P(x,t) = -\int \frac{\nabla\cdot F(\tau)\cdot\delta\left(t-\tau-\frac{|x-x_s|}{c_0}\right)}{4\pi|x-x_s|}\,d\tau = -\nabla\cdot\left(\frac{F(\tau_{ret})}{4\pi|x-x_s|}\right)$$ Set $r = |x-x_s|$

Algebra:

$$-\frac{\partial}{\partial x_i}\left(\frac{F_i(\tau_{ret})}{4\pi r}\right) = -\frac{1}{4\pi r}\cdot\frac{\partial F_i(\tau_{ret})}{\partial x_i} + \frac{1}{4\pi r^2}F_i(\tau_{ret})\frac{\partial r}{\partial x_i}$$

$$\frac{\partial r}{\partial x_i} = \frac{x_i}{r} = \hat{r}_i$$

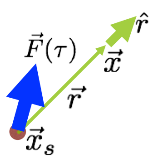

Algebra continued:

$$\frac{\partial F_i(\tau_{ret})}{\partial x_i} = \frac{\partial F_i(\tau_{ret})}{\partial \tau_{ret}}\cdot\frac{\partial \tau_{ret}}{\partial x_i} = -\frac{\partial F_i(\tau_{ret})}{\partial \tau_{ret}}\cdot\frac{\hat{r}_i}{C_0}$$

$$\frac{\partial F_i(\tau_{ret})}{\partial t} = \frac{\partial F_i(\tau_{ret})}{\partial \tau_{ret}}\cdot\underbrace{\frac{\partial \tau_{ret}}{\partial t}}_{1} = \frac{\partial F_i(\tau_{ret})}{\partial \tau_{ret}}$$

$$-\frac{\partial}{\partial x_i}\left(\frac{F_i(\tau_{ret})}{4\pi r}\right) = -\frac{1}{4\pi r}\cdot\frac{\partial F_i(\tau_{ret})}{\partial x_i} + \underbrace{\frac{1}{4\pi r^2}F_i(\tau_{ret})\frac{\partial r}{\partial x_i}}_{\text{Near field}}$$

$r \rightarrow \infty$

$$\boxed{\frac{\partial F_i(\tau_{ret})}{\partial x_i} = -\frac{\hat{r}_i}{C_0}\,\frac{\partial F_i(\tau_{ret})}{\partial t}}$$

Neglect near field term

$$-\frac{\partial}{\partial x_i}\left(\frac{F_i(\tau_{ret})}{4\pi r}\right) = \frac{1}{4\pi C_0 r}\cdot\frac{\partial F_i(\tau_{ret})}{\partial t}\hat{r}_i$$

$$\boxed{P(x,t) = \frac{1}{4\pi C_0 r}\cdot\frac{\partial F_i(\tau_{ret})}{\partial t}\hat{r}_i}$$

Now we can extend the vector to polar coordinates:

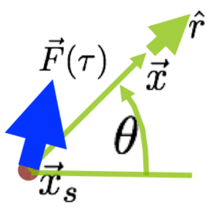

$$p(r,\theta,t) = \int_{-l/2}^{l/2}\frac{1}{4\pi C_0 r}\cdot\frac{\partial F_i(\tau_{ret})}{\partial t}\hat{r}_i\,dy \qquad \begin{cases} F_x = -D = -\frac{1}{2}\rho_0 U_0^2 C_d\, d \\ F_y = -L = -\frac{1}{2}\rho_0 U_0^2 C_l\, d \end{cases}$$

$$p(r,\theta,t) = \frac{\rho_0\cdot U_0^2\cdot d}{8\pi\cdot C_0\cdot r}\left(\sin(\theta)\int_{-l/2}^{l/2}\dot{C}_l(\tau_{ret})\,dy + \cos(\theta)\int_{-l/2}^{l/2}\dot{C}_d(\tau_{ret})\,dy\right)$$

$$C_l(\tau) = C_{l\,max}\,e^{-i(2\pi f_0\tau + \tilde{\varphi}_l(y))}$$
$$C_d(\tau) = C_{d\,max}\,e^{-i(2\pi 2f_0\tau + \tilde{\varphi}_d(y))}$$

Using these for integration

$$p(r,\theta,t) \simeq \frac{i\rho_0 U_0^2 d f_0 C_{l\,max}\sin(\theta)}{4C_0 r}e^{-i2\pi f_0(t-\frac{r}{C_0})}\cdot\int_{-l/2}^{l/2}e^{-i\tilde{\varphi}_l(y)}\,dy \qquad \eta = \frac{y}{l}$$

$$p(r,\theta,t) \simeq \frac{i\rho_0 U_0^2 d l f_0 C_{l\,max}\sin(\theta)}{4C_0 r}e^{-i2\pi f_0(t-\frac{r}{C_0})}\cdot\int_{-l/2}^{l/2}e^{-i\tilde{\varphi}_l(\eta)}\,d\eta$$

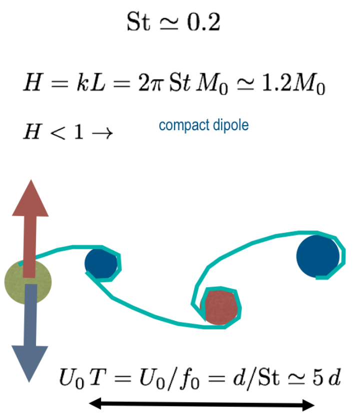

Acoustic Intensity

lets compute acoustic intensity for a harmonical signal:

$$I = \frac{(\hat{p}/\sqrt{2})^2}{\rho_0 C_0} \qquad St = \frac{f\cdot d}{U_0} \qquad I(r,\theta) = \frac{\rho_0 C_0^3 St^2 M_0^6 C_{l\,max}^2\sin^2(\theta)\,l^2}{32 r^2}\psi$$

where:

$$\psi = \int_{-l/2}^{l/2}\int_{-l/2}^{l/2}e^{-i[\tilde{\varphi}_l(\eta_1)-\tilde{\varphi}_l(\eta_2)]}\,d\eta_1\,d\eta_2$$

If the correlation length is small compared to l.

$$\psi = \int_{-\infty}^{\infty}R(\eta)\,d\eta$$

$$R(\eta) = \int_{-l/2}^{l/2}e^{-i[\tilde{\varphi}_l(\eta_1)-\tilde{\varphi}_l(\eta_2)]}\,d\eta_1$$

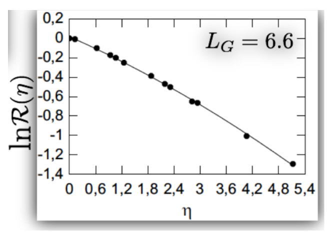

$$\begin{cases} R(\eta) = e^{-\frac{\eta^2}{2L_G^2}} & \psi = \sqrt{2\pi}\,L_G \\ R(\eta) = e^{\frac{|\eta|}{2L_E}} & \psi = 2L_E \end{cases}$$

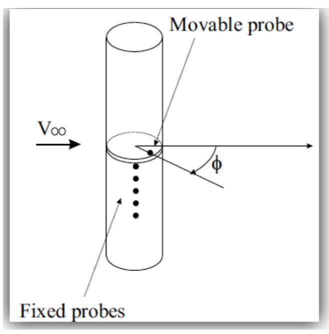

Results:

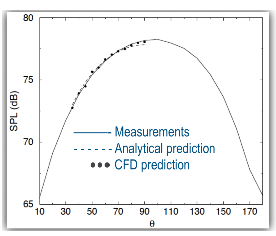

Basic Definitions

Acoustics: science of sound generation and propagation.

Human hearing: 20Hz – 20kHz

Aeroacoustics: sound generated aerodynamically

Sound: pressure perturbation that propagates in a fluid according to a wave motion

Sound pressure disturbance: $p'(t) = p(t) - p^0$ where: $p^0 = \bar{p} = \lim_{T \to \infty} \frac{1}{T} \int_{-T/2}^{T/2} p(t+t')\,dt'$

An appropriate measure of the strength of a signal is the root mean square: $\tilde{p} = \sqrt{\overline{(p')^2}}$

Definition of RMS: root mean square

$$f_{rms} = \lim_{T \to \infty} \sqrt{\frac{1}{T} \int_0^T [f(t)]^2\,dt}$$

Sinusoidal wave

$$\tilde{p} = \sqrt{1/2}\;\hat{p}$$

Threshold hearing: $\tilde{p}_{min} \approx 10^{-5}\,Pa$

Threshold pain: $\tilde{p}_{max} \approx 10^{2}\,Pa$

Logarithmic scale is used due to large range:

Sound Pressure Level (SPL): $L_p = 10 \log\left(\frac{\tilde{p}}{p_{ref}}\right)^2 = 20 \log\left(\frac{\tilde{p}}{p_{ref}}\right) dB$

$p_{ref} = 2 \cdot 10^{-5}\,Pa$

Doubling the p_{rms} corresponds to a 6.02 increase in SPL

Logarithmic scale of intensity and power

Sound Intensity:

$$I(x) = \overline{p'v'}$$

Sound Intensity Level

$$L_I = 10 \log\left(\frac{|I|}{I_{ref}}\right) \qquad [L_I] = dB \text{ (decibel)}$$

$$I_{ref} = 10^{-12}\,W/m^2$$

Sound Power

$P = \oint_A I \cdot n\,dA$ in a quiescent fluid (medium at rest)

Sound Power Level

$$L_W = 10 \log\left(\frac{P}{P_{ref}}\right) \qquad L_W = dB \text{ (decibel)}$$

$$P_{ref} = 10^{-12}\,W$$

Sound level perception

Affected by frequency. Two pure tones of same SPL are perceived at different loudness

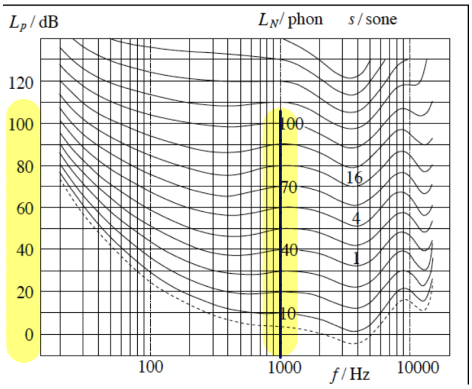

The loudness level L_N of pure tone of a pure tone is defined as the SPL at 1kHz.

Noise weighting: hearing sensitivity into account, SPL L_p is weighted in frequency-dependent way:

$L_{pA} = L_p + \Delta L_A$ (A-weighting

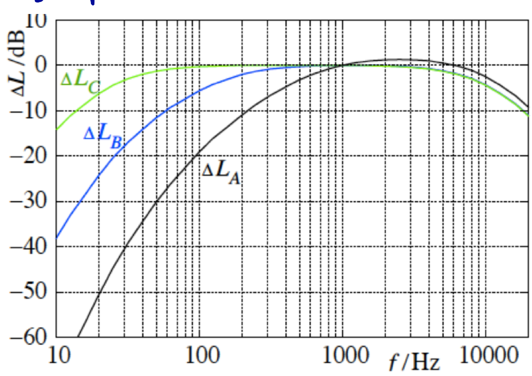

Ensemble Average

A process $p(t)$, the average over time.

$$\langle p \rangle (t) = \lim_{N \to \infty} \frac{1}{N} \sum_{n=0}^{N} P_n(t)$$

Statistically Stationary Process // Autocorrelation Function

P is the auto-correlation and t and Δt are arbitrary time shifts

$$P(\tau) = \langle p'(t) p'(t+\tau) \rangle = \langle p'(t+\Delta t) p'(t+\tau+\Delta t) \rangle$$

Typically $P(\tau)$ decays to 0 for large τ (forget the past)

We can split the signal into segments of duration Δt and consider this segments as independent realizations of the process. Ergodic

Fourier Transform: use to analyze on frequency domain.

A statistically stationary random process is conveniently analyzed in the frequency domain through the fourier transform.

$$\hat{h}(\omega) = \int_{-\infty}^{\infty} h'(t) \exp(-i\omega t)\, dt$$ $\longrightarrow$ only works if $h'(t)$ is square integrable $\int_{-\infty}^{\infty} |h'(t)|^2 dt < \infty$

$i = \sqrt{-1}$ $\quad f = \frac{\omega}{2\pi}$

A signal can be recovered by the sumation of the spectral components with the inverse Fourier transform

$$h'(t) = \frac{1}{2\pi} \int_{-\infty}^{\infty} \hat{h}(\omega) \exp(i\omega t)\, d\omega$$

Autocorrelation + Fourier Transform:

Autocorrelation function: $P(\tau) = \langle p'(t) p'(t+\tau) \rangle$ Is square integrable if it decays to zero sufficiently fast for large values τ. We can use the fourier transform.

$$\hat{P}(\omega) = \int_{-\infty}^{\infty} P(\tau) \exp(-i\omega\tau)\, d\tau$$ and the inverse $$\tilde{P}^2 = P(\tau=0) = \int_{-\infty}^{\infty} \hat{P}(\omega) \frac{d\omega}{2\pi} = \int_{-\infty}^{\infty} \hat{P}(f)\, df$$

Energy Integral Division: Bands

We can divide the energy integral in bands and compute the energy for every band. $\tilde{P}_i^2 = \int_{f_i^l}^{f_i^u} \hat{P}(f)\, df$

The bands are defined by a lower, an upper and a central frequency: $\Delta f_i = f_i^u - f_i^l$ $\quad$ energy is preserved: $\tilde{P}^2 = \sum_{-\infty}^{\infty} \tilde{P}_i^2$

Constant Narrow Bands (tipically as directly from Discrete Fourier Transform)

$\Delta f_i = \Delta f = \text{constant}$ $\qquad f_i^c = (f_i^l + f_i^u)/2 = f_0^c + i\Delta f$

Band Sound Pressure Level $L_p^i = 20 \log(\tilde{P}_i(f_i^c)/P_{ref})$

$\frac{f_i^u}{f_i^l} = 2^m = \text{constant}$ $\quad f_i^c = (f_i^l f_i^u)^{1/2}$ $\quad \Delta f_i = (2^{m/2} - 2^{-m/2}) f_i^c$

- $m = 1$ octave band
- $m = 1/3$ one-third octave band
- $m = 1/12$ one twelfth octave band

central frequencies: $f_i^c = (f_i^l f_i^u)^{1/2} = 2^{mi} f_0^c$ reference central frequency $\rightarrow f_0^c = 1\,kHz$

White Noise: Octave band linearly increases by 3dB band, 1/3 band increases by 1dB/band

Wave Theory of Sound

Flow governing equations in conservative form:

$$\frac{\partial \rho}{\partial t} + \nabla \cdot (\rho v) = \dot{m}$$ Conservation of mass

$$\frac{\partial \rho v}{\partial t} + \nabla \cdot (\rho v v) + \nabla p = \nabla \cdot \tau + f + \dot{m} v$$ Conservation of linear momuentum

$$\frac{\partial \rho e_t}{\partial t} + \nabla \cdot (\rho e_t v) + \nabla \cdot (p v) = -\nabla \cdot q + \nabla \cdot (\tau v) + \dot{\vartheta} + f \cdot v + \dot{m} e_t$$ Conservation of total energy

ρ = density, v = velocity, p = pressure, e_t = specific total energy, $\dot{m}$ = local injection rate, f = local force per unit of volume

$\dot{\vartheta}$ = local heating rate

Constitutive Relationships

$e_t = e + \frac{1}{2}v^2 \qquad e = C_v \cdot T$ especific internal energy.

dynamic viscosity

$\tau = \mu(\nabla v + {}^t\nabla v - \frac{2}{3}I\nabla\cdot v)$, $\tau_{ij} = \mu\left(\frac{\partial v_i}{\partial x_j} + \frac{\partial v_j}{\partial x_i}\right) - \frac{2}{3}\mu\left(\frac{\partial v_k}{\partial x_k}\right)\delta_{ij}$ → $\begin{cases}\delta_{ij} = 1 \text{ if } i=j \\ \delta_{ij} = 0 \text{ if } i\neq j\end{cases}$

$q = -k\nabla T$ fourier law of heat conduction $\quad P = \rho R T$ perfect gas law

More terms:

$C_p = R + C_v$ specific heat capacity at constant pressure

$\gamma = C_p/C_v$ with e.g. $\gamma \approx 1.4$ for air specific heat ratio

Entropy: S Gibbs Relationship

$T\delta s = \delta e - (P/\rho^2)\delta\rho$ for a perfect gas: $S = S_r + C_v \cdot \log\left(\frac{P}{P_r}\right)\left(\frac{\rho_r}{\rho}\right)^{\gamma}$ → reference state

Derive the following differential relationship: $\delta s = C_v\left(\frac{\delta P}{P} - \gamma\frac{\delta\rho}{\rho}\right)$ (1)

For any isentropic perfect gas transformation process $S = \text{constant} \rightarrow P = k\rho^{\gamma}$

$\rho = \rho(P,s)$ in differential form

$$\delta\rho = \underbrace{\left(\frac{\partial\rho}{\partial P}\right)_s}_{=1/a^2}\delta P + \underbrace{\left(\frac{\partial\rho}{\partial s}\right)_P}_{=-\rho\sigma}\delta s$$

where from the isentropic law $a^2 = \gamma R T = \gamma\cdot\frac{P}{\rho}$ $\qquad$ from (1) $\sigma = \frac{1}{C_p}$

Linearization: $(\rho, v, P, a^2, \sigma, \dots) = (\rho^0 + \varepsilon\rho', v^0 + \varepsilon v', P^0 + \varepsilon P', (a^2)^0 + \varepsilon(a^2)', \sigma^0 + \varepsilon\sigma', \dots)$

- $\frac{D\rho}{Dt} = -\rho\nabla\cdot v + \dot m$
- $\rho\frac{Dv}{Dt} = -\nabla P + \nabla\tau + f$
- $\rho\frac{De}{Dt} = -P\nabla\cdot v + \tau : \nabla v - \nabla\cdot q + \dot\theta$
- $\rho\frac{Ds}{Dt} = \frac{1}{T}\left[\tau : \nabla v - \nabla q + \dot\theta - \dot m\frac{P}{\rho}\right]$
- $\frac{1}{a^2}\frac{DP}{Dt} = -\rho\nabla\cdot v + \frac{\sigma}{T}(\tau : \nabla v - \nabla q + \dot\theta) + \dot m\left(1 - \frac{\sigma}{T}\frac{P}{\rho}\right)$

- Acoustics describes propagation of small distur.
- It is an inherently unsteady phenomenon
- Any quality can be splited into:
  $P = P^0 + \varepsilon P' \quad \varepsilon \ll 1$
- Steady mean flow:
  $\dot m^0 = 0,\ f^0 = 0,\ \dot\theta^0 = 0$
- Neglect the effects of viscous stresses fluctuations and heat conduction.

Linearize equations:

$$\frac{D^0\rho'}{Dt} + \rho^0\nabla\cdot v' + v'\cdot\nabla\rho^0 + \rho'\nabla\cdot v^0 = \dot m'$$

$$\frac{D^0}{Dt} = \frac{\partial}{\partial t} + v^0\cdot\nabla$$

$$\rho^0\frac{D^0 v'}{Dt} + \nabla P' + \rho^0 v'\cdot\nabla v^0 + \rho' v^0\cdot\nabla v^0 = f'$$

$$\underbrace{\frac{1}{(a^2)^0}}_{\left[\rho^0/\gamma P^0\right]_P}\left(\frac{D^0 P'}{Dt} + v'\cdot\nabla P^0\right) + \rho^0\nabla\cdot v' + \underbrace{\left(\rho^0\frac{(a^2)'}{(a^2)^0} + \rho'\right)}_{\left[\frac{\gamma}{(a^2)^0}P'\right]_P}\nabla\cdot v^0 = \overbrace{\frac{\sigma^0}{T^0}\dot\theta' + \left(1 - \frac{\sigma^0}{\rho^0}\cdot\frac{P^0}{T^0}\right)\dot m'}^{\left[\frac{\gamma-1}{(a^2)^0}\dot\theta' + \frac{1}{\gamma}\dot m'\right]_P}$$

ACOUSTC EQUATION FOR A MEDIUM AT A REST $v^o = 0$ $P^o = \text{constant} = P_\infty$ $\rho^o = \rho^o(x)$

$$\left.\begin{aligned} &\frac{\partial \rho'}{\partial t} + v'\nabla\rho^o + \rho^o \nabla v' = \dot{m}' \\ &\rho^o \frac{\partial v'}{\partial t} + \nabla p' = f' \\ &\frac{1}{(a^2)^o}\frac{\partial p'}{\partial t} + \rho^o \nabla\cdot v' = \dot{\theta}' \end{aligned}\right\} \quad \frac{1}{(a^2)^o}\frac{\partial^2 p'}{\partial t^2} - \rho^o \nabla\cdot\left(\frac{1}{\rho^o}\nabla p'\right) = Q_p$$

$$Q_p = \underbrace{\left(1 - \frac{\sigma^o}{\rho^o}\cdot\frac{P_\infty}{T^o}\right)\frac{\partial \dot{m}'}{\partial t} + \frac{\sigma^o}{T^o}\cdot\frac{\partial\dot{\theta}'}{\partial t}}_{\left[\frac{\gamma-1}{(a^2)^o}\frac{\partial\dot{\theta}'}{\partial t} + \frac{1}{\gamma}\frac{\partial \dot{m}'}{\partial t}\right]_{Pg}} - \rho^o\nabla\cdot\left(\frac{1}{\rho^o}f'\right)$$

ACOUSTIC EQUATION ASSUMING COSTANT MEAN FLOW DENSITY

$$\frac{1}{(a^2)_\infty}\frac{\partial^2 p'}{\partial t^2} - \Delta p' = Q_p \qquad Q_p = \underbrace{\left(1 - \frac{\sigma_\infty\cdot P_\infty}{\rho_\infty\cdot T_\infty}\right)\cdot\frac{\partial\dot{m}'}{\partial t} + \frac{\sigma_\infty}{T_\infty}\cdot\frac{\partial\dot{\theta}'}{\partial t}}_{\left[\frac{1}{\gamma}\cdot\frac{\partial\dot{m}'}{\partial t} + \frac{\gamma-1}{(a^2)_\infty}\frac{\partial\dot{\theta}'}{\partial t}\right]_{Pg}} - \nabla\cdot f'$$

$\nabla\nabla = \Delta$ laplacian

a_∞ speed of sound

Force acts as a dipole

In f-domain $-k^2\hat{p} - \Delta\hat{p} = \hat{Q}_p$

$$k = \frac{\omega}{a}$$

INTENSITY, POWER, ENERGY CONSERVATION

$$\rho^o\frac{\partial v'}{\partial t} + \nabla p' = f' \xrightarrow{\text{multiply by } v'} \frac{\partial}{\partial t}\left(\rho^o\cdot\frac{1}{2}v'^2\right) + v'\cdot\nabla p' = v'\cdot f'$$

$$\frac{1}{(a^2)^o}\frac{\partial p'}{\partial t} + \rho^o\nabla\cdot v' = \dot{\theta}' \xrightarrow{\text{multiply by } p'/\rho^o} \frac{\partial}{\partial t}\left(\frac{\frac{1}{2}p'^2}{\rho^o(a^2)^o}\right) + p'\nabla\cdot v' = \frac{1}{\rho^o}\dot{\theta}'p'$$

Adding them both:

$$\frac{\partial}{\partial t}\left(\rho^o\cdot\frac{1}{2}v'^2 + \frac{\frac{1}{2}p'^2}{\rho^o(a^2)^o}\right) + \nabla\cdot(p'v') = v'\cdot f' + \frac{1}{\rho^o}\dot{\theta}'p'$$

Integrating over a volume V containing all the sources

$$\int_V \frac{\partial E}{\partial t}\,dV + \int_V \nabla\cdot(p'v')\,dV = \int_V Q\,dV$$

Assuming a steady V and using Gauss theorem

$$\frac{d}{dt}\int_V E\,dV + \oint_{\partial V}(p'v')\cdot n\,dA = \int_{V_s} Q\,dV$$

$I = p'\cdot v'$ is the acoustic intensity.

Sound Power on periodic signal and taking the time-average over a period:

$$0 + \oint_{\partial V} I\cdot n\,dA = \int_{V_s}\bar{Q}\,dV = P$$

Acoustic Analogies

We have to predict noise in the far field. How do we predict it?

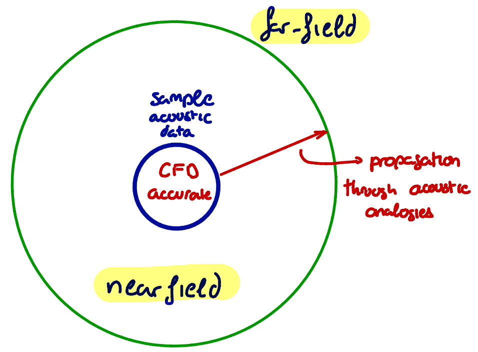

Full CFD:

- accurate
- expensive
- large domains
- high acustic resolution

Hybrid CFD/CAA

- high accurate CFD near field
- less expensive
- Small domains
- High resolution only near field

Separate the sound generation from propagation

Formulation of Acoustic Analogies

Flow governing equations ⟶ Wave equation: propagation + source term ⟶ Depending on the ref. wave equation and source we can have diff formulation

- → Lighthill: turbulent flow in a quiescent environment
- → Ffowcs Williams and Hawkings: extension to flow confined by surfaces in arbitrary motion.

Source Information

Solid

- Integration of pressure field over the physical surface of the body
- Confines all the flow non-linearity in a volume integral over a domain exterior to a body

Permeable

- Integration of the pressure field over a control surface
- Includes also the non-linear (quadropole) sources inside surface
- The control surface shall be placed in a linear flow region.

The Ffowcs Williams and Hawkings Analogy

The FWH analogy accounts for movement (such as propelles or rotors)

The flow enclosed by the surface $f(x,t) < 0$, can be replaced by a quiescent fluid and a surface distribution of sources which restore the conservative character of the field.

$\rho_0, P_0, u = 0$

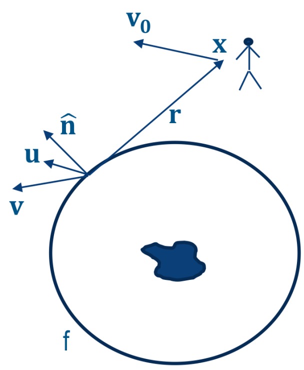

surface source distribution of mass

$$\frac{\partial}{\partial t}\left[(\rho-\rho_0)H(f)\right] + \frac{\partial}{\partial x_i}\left[\rho u_i H(f)\right] = Q\,\delta(f) \quad \text{continuity equation}$$

heaviside function

$$\frac{\partial}{\partial t}\left[\rho u_i H(f)\right] + \frac{\partial}{\partial x_i}\left[(\rho u_i u_j + P_{ij})H(f)\right] = \underbrace{L_i\,\delta(f)}_{\text{Surface source distribution of momentum}} \quad \text{momentum equation}$$

$f(x,t) = 0$ control surface that moves with velocity $v(x,t)$

$\hat{n}$ normal vector to the surface — u velocity of the flow

v velocity of integration surface — v_0 listener velocity.

$$Q = \rho_0 U_i \hat{n}_i \qquad L_i = P_{ij}\hat{n}_j + \rho u_i (u_n - v_n)$$

$$U_i = \left(1 - \frac{\rho}{\rho_0}\right) v_i + \frac{\rho}{\rho_0} u_i \qquad P_{ij} - (p - p_0)\delta_{ij} + \tau_{ij}$$

A flow field is conservative if and only if exist a function f such that $F = \text{Grad} f$

As long as the net mass flow is zero, a body with closed shape might be represented.

CONTINUED

$$\frac{\partial H(f)}{\partial t} = \delta(f)\frac{\partial f}{\partial t} = \delta(f)\, V_n$$

$$\frac{\partial H(f)}{\partial x_i} = \delta(f)\frac{\partial f}{\partial x_i} = \delta(f)\,\hat{n}$$

The continuity and momentum equation can be rewritten in form of a standard wave equation that describes the propagation of an acoustic disturbance p' in a quiescent environment

$$\underbrace{\Box^2}_{\text{wave operator}} p' = \left(\frac{1}{c^2}\frac{\partial}{\partial t^2} - \nabla^2\right)p' = 0$$

Substract the divergence of the continuity equation to the time derivative of the linear momentum equation

FWH equation:

$$\Box^2\left[(\rho-\rho_0)\,c^2 H(f)\right] = \frac{\partial^2}{\partial x_i \partial x_j}\left[T_{ij} H(f)\right] - \frac{\partial}{\partial x_i}\left[l_i\,\delta(f)\right] + \frac{\partial}{\partial t}\left[Q\,\delta(f)\right]$$

Stress tensor

$$T_{ij} = \rho u_i u_j + (p' - c^2\rho')\,\delta_{ij} - \tau_{ij}$$

Assume small density perturbations: INHOMOGENEOUS WAVE EQUATION FOR PRESSURE

$$\Box^2\left[p' H(f)\right] = \underbrace{\frac{\partial^2}{\partial x_i \partial x_j}\left[T_{ij} H(f)\right]}_{\text{Quadropole source term}} \overbrace{- \frac{\partial}{\partial x_i}\left[l_i\,\delta(f)\right]}^{\text{Loading source term:}} + \underbrace{\frac{\partial}{\partial t}\left[Q\,\delta(f)\right]}_{\text{Thickness source term}}$$

Volume distribution of sources — Surface distribution of sources

Quadropole source term: accounts for flow non-linearities in the domain exterior to the control surfaces. (Shock waves, vortical disturbances)

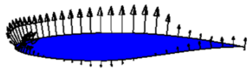

Loading source term: accounts for unsteady loading exerted by the body on the fluid.

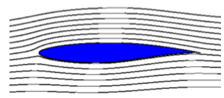

Thickness source term: accounts for the fluid displacement produced by the body motion.

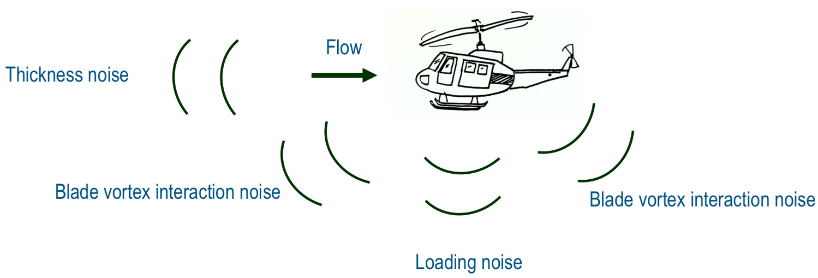

GREEN'S FUNCTION

Impulse response of an inhomogeneous linear differential equation defined on a domain with specified initial condition or boundary condition.

$$\underbrace{L}_{\text{Operator}}\overbrace{\phi(x)}^{\text{Function}} = \underbrace{f(x)}_{\text{other function}}$$

If $L g(x) = \delta(x) \longrightarrow \phi(x) = \int f(x')\, g(x-x')\, d^3x'$

RETARDED-TIME SOLUTION OF THE FWH ANALOGY

The computational time is now the reception time. It evaluates the signal received at a given time t through simulation of all the disturbances reaching the observer at the same time t. These are emitted at different retarded times and cover different distances before reaching the observation point.

$$\square^2 [p' H(f)] = \frac{\partial^2}{\partial x_i \partial x_j}[T_{ij} H(f)] - \frac{\partial}{\partial x_i}[l_i \delta(f)] + \frac{\partial}{\partial t}[Q \delta(f)]$$

The green equation in this case is:

$$G = \frac{\delta(g)}{r} \quad \text{where} \quad g = t - \tau - \frac{r}{c} \qquad r = |x - y|$$

τ → Source emission time

t → observer reception time

Applying green's equation:

$$4\pi p' = \frac{\partial^2}{\partial x_i \partial x_j}\iint_{f>0} \frac{\delta(t-\tau-r/c)}{r} T_{ij}\, dV d\tau - \frac{\partial}{\partial x_i}\iint_{f=0} \frac{\delta(t-\tau-r/c)}{r} l_i \, dS d\tau + \frac{\partial}{\partial t}\iint_{f=0} \frac{\delta(t-\tau-r/c)}{r} Q \, dS d\tau$$

Applying a change of variables and considering that:

$$\int F(\tau)\delta(g(\tau)) = \sum_{n=1}^{N} \frac{F(\tau_n^*)}{\partial g/\partial \tau}$$

where the sum is taken all over the roots τ_n^* on the retarded time equation $g = 0$ and $\frac{\partial g}{\partial \tau} = -1 + M_r$ where $M_r = M_i \hat{r}_i$ is the component of the source Mach number vector in the direction of the observer $\hat{r}_i = (x_i - y_i)/r$

$F(\tau_n^*)$: When source is in subsonic motion, only one solution of retarded time equation. If supersonic motion, more than one. This is due to impulses at different times can be perceived at the same time

$\partial g/\partial \tau$: $|1 - M_r|$ accounts for a dilatation or contraction of the observer time scale w.r.t the source time scale : Doppler effect.

Assuming subsonic flow motion and the retarded time.

$$\tau^* = t - \frac{|x - y(\tau^*)|}{c}$$ the solution can be rewritten:

$$4\pi p' = \frac{\partial^2}{\partial x_i \partial x_j}\int_{f>0}\left[\frac{T_{ij}}{r(1-M_r)}\right]_{ret} dV - \frac{\partial}{\partial x_i}\int_{f=0}\left[\frac{l_i}{r(1-M_r)}\right]_{ret} dS + \frac{\partial}{\partial t}\int_{f=0}\left[\frac{Q}{r(1-M_r)}\right]_{ret} dS$$

singularity can be removed with a different change of variables

Change space derivatives to time derivatives:

$$\frac{\partial}{\partial x_i}\int_{f=0}\left[\frac{l_i}{r(1-M_r)}\right]_{ret} dS = -\frac{1}{c}\frac{\partial}{\partial t}\int_{f=0}\left[\frac{l_i \hat{r}_i}{r(1-M_r)}\right]_{ret} dS - \left[\frac{l_i \hat{r}_i}{r^2(1-M_r)}\right]_{ret} dS$$

$$4\pi p' = \frac{1}{c^2}\frac{\partial^2}{\partial t^2}\int_{f>0}\left[\frac{T_{rr}}{r(1-M_r)}\right]_{ret} dV + \frac{1}{2}\frac{\partial}{\partial t}\int_{f>0}\left[\frac{3T_{rr}-T_{ij}}{r^2(1-M_r)}\right]_{ret} dV + \int_{f>0}\left[\frac{3T_{rr}-T_{ij}}{r^3(1-M_r)}\right]_{ret} dV + \frac{1}{c}\frac{\partial}{\partial t}\int_{f=0}\left[\frac{l_i\hat{r}_i}{r(1-M_r)}\right]_{ret} dS + \int_{f=0}\left[\frac{l_i\hat{r}_i}{r^2(1-M_r)}\right]_{ret} dS + \frac{\partial}{\partial t}\int_{f=0}\left[\frac{Q}{r(1-M_r)}\right]_{ret} dS$$

Moving the time derivative within the integral

$$\left.\frac{\partial}{\partial t}\right|_x = \left[\frac{1}{1-M_r}\left.\frac{\partial}{\partial \tau}\right|_x\right]_{ret}$$

$\square|_x$: derivative taken at fixed observer position and using

$$\frac{\partial r}{\partial \tau} = -cM_r \qquad \frac{\partial \hat{r}_i}{\partial \tau} = \frac{\hat{r}_i c M_r - cM_i}{\tau} \qquad \frac{\partial M_r}{\partial \tau} = \frac{1}{\tau}\left[r\hat{r}_i\frac{\partial M_i}{\partial \tau} + c\left(M_r^2 - M^2\right)\right]$$

The retarded time equation can be written as:

$$p'(x,t) = \underbrace{p'_Q(x,t)}_{\text{Thickness}} + \underbrace{p'_L(x,t)}_{\text{Loading}} + \underbrace{p'_T(x,t)}_{\text{Quadrupole}}$$

ADVANCED-TIME SOLUTION

The computational time is the emission time, consists in using a retarded time approach but the point of view of the source. At each computational time and for each source element, the time at which the disturbance will reach the observer.

retarded time equation:

$$\tau_{ret} = t - \frac{|x(t) - y(\tau_{ret})|}{c} \quad \text{retarded time equation}$$

at an observer time $t+T$

$$\tau'_{ret} = t + T - \frac{|x(t+T) - y(\tau_{ret}')|}{c}$$

time at which a disturbance emitted at y will reach the observer.

Setting $\tau'_{ret} \equiv t$

$$T = \frac{|x(t+T) - y(t)|}{c}$$

If the observer moves at constant velocity cM_0, then:

$$T^{\pm} = \frac{r_i M_{0i} \pm \sqrt{(r_i M_{0i})^2 + r^2(1-M_0^2)}}{c(1-M_0^2)} = \frac{r}{c}\left(\frac{M_{0r} \pm \sqrt{M_{0r}^2 + 1 - M_0^2}}{(1-M_0^2)}\right)$$

radiation vector

The signal cannot be perceived before being emitted

Radiation Mach number

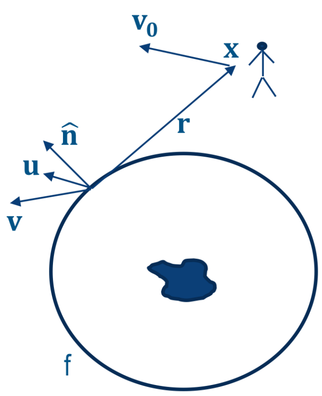

Supersonic motion:

If observer moves close to source, solution physically acceptable

If observer moves away from source, solution is physically unacceptable

Propeller Noise

Assumptions

- Low tip Mach number:
- Noise generations by blade loadings of open (unducted) rotors.
- Only constantly-spaced blade systems are used in frequency domain.
- Only formulas for Tonal Noise contributions due to periodic wake/stator and or rotation are derived
- TE broadband formulas (next lecture)
- Same sound generation mechanisms are the same: R_0, Ω, B specific design challenges and methods.
- Rotor operates in ideal unperturbed flow conditions No turbulence - blade interaction.

Farasat Formulation 1A, subsonic moving sources

Thickness noise:

$$4\pi p'_T(x,t) = \int_{f=0}\left[\frac{\rho_0\left(\dot U_n + U_{\dot n}\right)}{r\left(1-M_r\right)^2}\right]_{ret} dS + \int_{f=0}\left[\frac{\rho_0 U_n\left(r\dot M_r + c\left(M_r - M^2\right)\right)}{r^2\left(1-M_r\right)^3}\right]_{ret} dS$$

$$U_i = \left(1-\frac{\rho}{\rho_0}\right)v_i + \frac{\rho u_i}{\rho_0}$$

v: surface velocity

u: flow velocity

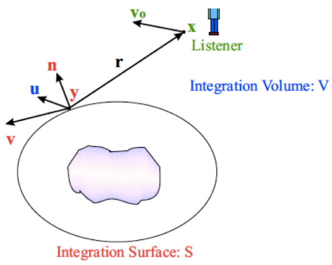

Where M is the Mach number vector of a source point on the integration surface, the remaining terms are:

$$U_n = U_i \hat n_i, \quad U_{\dot n} = U_i \dot{\hat n}_i, \quad \dot U_n = \dot U_i \hat n_i, \quad M_r = M_i \hat r_i, \quad \dot M_r = \dot M_i \hat r_i$$

Dots on quantities denote time derivatives with respect to the source time τ.

Loading Noise

$$4\pi p'_L(x,t) = \frac{1}{c}\int_{f=0}\left[\frac{\dot L_r}{r\left(1-M_r\right)^2}\right]_{ret} dS + \int_{f=0}\left[\frac{L_r - L_M}{r^2\left(1-M_r\right)^2}\right]_{ret} dS + \frac{1}{c}\int_{f=0}\left[\frac{L_r\left(r\dot M_r + c\left(M_r - M^2\right)\right)}{r^2\left(1-M_r\right)^3}\right]_{ret} dS$$

$$L_i = P_{ij}\hat n_j + \rho u_i\left(u_n - v_n\right) \qquad L_r = L_i \cdot \hat r_i \qquad \dot L_r = \dot L_i \hat r_i \qquad L_M = L_i M_i$$

$$P_{ij} = \left(p - p_0\right)\delta_{ij} - \tau_{ij}$$

RETARDED TIME VS ADVANCED TIME FORMULATION

$[\cdots]_{ret}$ evaluation at the retarded time

$$\tau_{ret} = t - \frac{|x(t) - y(\tau_{ret})|}{c}$$

Implicit equations to be solved iteratively, up to 3 solutions for supersonic rotating sources. Doppler effect.

We can instead calculate the arrival time.

$$t_{adv} = t + T \qquad T = \frac{|x(t+T) - y(t)|}{c}$$

y = source point from here
x = observer to here

ON THE FLY IMPLEMENTATION

At the current time step k, for every discrete surface element j:

1. Use flow velocity, pressure and density to compute elementary contribution.
2. Evaluate the reception time $t^j_{k\,adv}$
3. Store the signal as a double array $(p, t_{adv})^j_k$
4. At the end of computation, sum up all transition signal through projection on a constant time step sequence.
5. Compute spectra:

   analysis (time domain) synthesis (frequency domain)

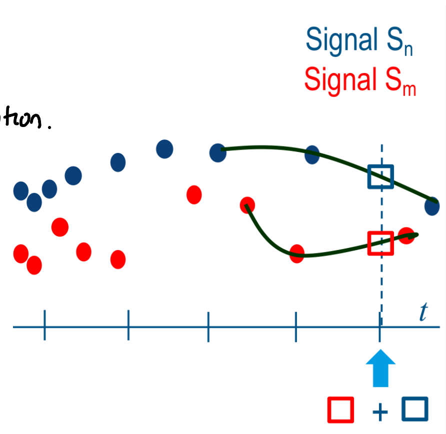

MONOPOLE

The doppler frequency shift and amplification can be illustrated by considering the acoustic field generated by a monopole of strength $Q(t)$ moving along $x = x_s(t)$ in a quiescent medium.

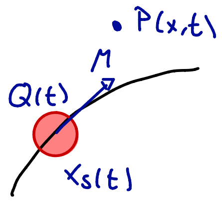

DERIVATION:

$$\frac{1}{c^2}\frac{\partial^2 p}{\partial t^2} - \nabla p' = \rho_0 \frac{\partial}{\partial t}\left\{Q(t)\,\delta(x - x_s(t))\right\}$$

After: green's function, evaluate y-integral, change of variable

$$p(x,t) = \rho_0 \frac{\partial}{\partial t}\int \frac{Q(\tau)\,\delta(t-\tau-|x-x_s(\tau)|/c)}{4\pi|x-x_s(\tau)|}\,d\tau \longrightarrow \int Q(\tau)\,\delta(g(\tau))\,d\tau = \sum_{n=1}^{N}\frac{Q(\tau_n^*)}{\left|\frac{\partial g}{\partial \tau}(\tau_n^*)\right|}$$

where:

$$g(\tau) = \frac{t - \tau - |x - x_s(\tau)|}{c} \qquad cM_r = V_s\cdot\hat{r} \qquad \hat{r}_i = \frac{x_i - x_{si}}{|x - x_s(\tau)|}$$

$$V_{si} = \frac{\partial x_{si}}{\partial \tau}$$

$$\frac{\partial g}{\partial \tau} = -1 + \frac{1}{c}\frac{x_i - x_{si}}{|x - x_s(\tau)|}\frac{\partial x_i}{\partial \tau} = -1 + M_r$$

Changes of variables and substitutions

$$p(x,t) = \rho_0 \sum_{n=1}^{N} \frac{\partial}{\partial t} \left\{ \frac{Q(\tau_n^*)}{4\pi |x - x_s(\tau_n^*)| |1 - M_r(\tau_n^*)|} \right\}$$

retarded time

$$\tau_n^* = t - |x - x_s(\tau_n^*)| / c$$

Relationship between emission and reception time:

$$\frac{\partial \tau_n^*}{\partial t} = \frac{1}{\underbrace{1 - M_r(\tau_n^*)}_{\text{doppler freq shift}}}$$

- Approaching subsonic $0 \le M_r \le 1$ $(1 - M_r)^{-1} \ge 1$ contraction and higher detected frequencies
- Receding subsonic $-1 \le M_r \le 0$ $0.5 \le (1 - M_r)^{-1} \le 1$ dilation and lower detected frequencies.
- Approaching supersonic $M_r > 1$ $(1 - M_r)^{-1} < 0$ signals emitted later are detected earlier.

Consider monopole moving subsonically, reception time into emission time

Accoustic pressure from subsonically moving monopole takes form:

$$p(x,t) = \frac{\rho_0}{4\pi} \left[\frac{\dot{Q}}{r(1 - M_r)^2} + \frac{Q}{r^2(1 - M_r)^3} \cdot \left\{ r\dot{M}_r + c(M_r - M^2) \right\} \right]_{ret} \qquad \dot{M}_r = \hat{r}_i \frac{\partial M_i}{\partial \tau}$$

Dipole

Force $F(t)$ moving in a quiescent medium. The radiated acoustic pressure is decribed by wave equation.

$$\frac{1}{c^2} \frac{\partial^2 p}{\partial t^2} - \nabla^2 p = \frac{\partial}{\partial x_i} \left\{ F_i(t) \, \delta(x - x_s(t)) \right\}$$

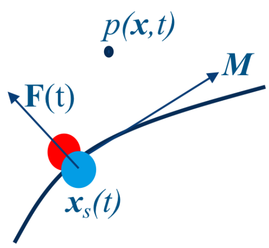

Solution is:

$$p(x,t) = \sum_{n=1}^{N} \frac{\partial}{\partial x_i} \left[\frac{F_i}{4\pi r \, |1 - M_r|} \right]_{ret}$$

Subsonic dipole: Higher order Döppler factors appear for higher multipoles.

$$4\pi \, p(x,t) = -\frac{1}{c} \left[\frac{\dot{F}_r}{r(1 - M_r)^2} \right]_{ret} - \frac{1}{c} \left[\frac{F_r \{ r\dot{M}_r + c(M_r - M^2) \}}{r^2 (1 - M_r)^3} \right]_{ret} - \left[\frac{F_r - F_M}{r^2 (1 - M_r)^2} \right]_{ret}$$

$\dot{F}_r = \dot{F}_i \hat{r}_i$

$F_M = F_i M_i$

Using emission-time derivatives has several advantages but results in transonic singularities due to doppler effect.

Compact monopole-dipole formulation

Geometry: fluid displacement, monopole contribution

Force: fluid loading, dipole contribution

If we are only interested in low frequency noise, such that $\lambda >> \text{chord}$ acoustically compact source

The blade can be replaced by an equivalent blade with the same spanwise load distribution and flow displacement

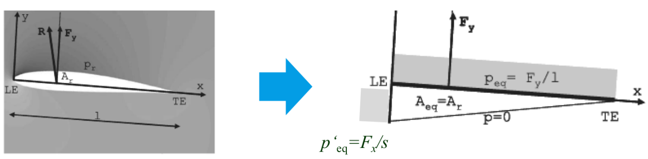

Rotating sources – frequency domain solutions (1/4)

Monopole

$$p(x,t) = \rho_0 \frac{\partial}{\partial t}\left[\frac{Q}{4\pi r(1-M_r)}\right]_{ret}$$

$$P_M(x,\omega) = -\frac{i\omega\rho_0}{4\pi}\int_{-\infty}^{\infty}\frac{Q(\tau)}{r(\tau)}e^{i\omega(\tau + r/c)}\,d\tau$$

Assume periodicity $= 0$

$t = \tau + \frac{r}{c} \quad dt = (1-M_r)\,\partial\tau$

Fourier:

$$P(x,\omega) = \int_{-\infty}^{\infty} p(x,t)\,e^{i\omega t}\,dt$$

Dipole

$$p(x,t) = -\frac{1}{c}\frac{\partial}{\partial t}\left[\frac{F_i \hat{r}_i/4\pi}{r|1-M_r|}\right]_{ret} - \left[\frac{F_i\hat{r}_i/4\pi}{r^2|1-M_r|}\right]_{ret}$$

$$P_D(x,\omega) = -\frac{1}{4\pi}\int_{-\infty}^{\infty}\frac{F_r(\tau)}{r(\tau)^2}(1-ikr)\,e^{-i\omega(\tau + r/c)}\,d\tau$$

Assume periodicity $= 0$

$t = \tau + \frac{r}{c}, \; dt = (1-M_r)\,\partial\tau$

Fourier:

$$p(x,t) = \frac{1}{2\pi}\int_{-\infty}^{\infty} P(x,\omega)\,e^{-i\omega t}\,d\omega$$

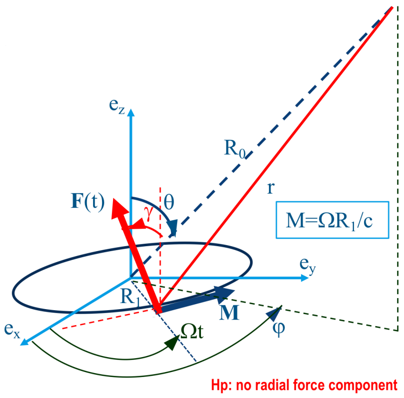

$X_M = [R_0\sin(\theta)\cos(\varphi),\, R_0\sin(\theta)\sin(\varphi),\, R_0\cos(\theta)]$

$X_S = [R_1\cos(\Omega t),\, R_1\cdot\sin(\Omega t),\, 0]$

$F = F\cdot(\sin(\gamma)\sin(\Omega t),\, \sin(\gamma)\cos(\Omega t),\, \cos(\gamma))$

$$F_r = \begin{cases} \text{if } R_1 \ll R_0\text{, geometrical far field} \\ \sim F R_0(\sin(\theta)\sin(\gamma)\sin(\Omega t - \varphi) + \cos(\theta)\cos(\gamma))/r \\ \text{else} \\ F(R_0\sin(\theta)\cos(\varphi)\sin(\gamma)\sin(\Omega t) - R_1\cos(\Omega t)\sin(\gamma)\sin(\Omega t) \\ \quad + R_0\sin(\theta)\sin(\varphi)\sin(\gamma)\cos(\Omega t) - R_1\sin(\Omega t)\sin(\gamma)\cos(\Omega t) \\ \quad + R_0\cos(\theta)\cos(\gamma))/r \end{cases}$$

Remarks

- Once $F(t)$ and $Q(t)$ are prescribed we can use exact or approximate expressions of $F_r(t)$ and $r(t)$ to compute the radiated noise in the frequency domain: with numerical integration.
- Time integral must be bound, boundaries not $-\infty$ and ∞, least common multiplier of $F(t)$ and $Q(t)$
- Numerical integration is not avoidable, time domain is preferred
- On frequency domain, we remove the singularity problem
- Frequency domain: good to derive analytical formulas, but chordwise compact and far field approx must be introduced ($\lambda \gg$ chord, $r \gg R_1$)

Analytical expression of far-field noise from a rotating force

Without radial force component:

$$P_D(x,\omega) \approx \frac{ik}{4\pi}\int_{-\infty}^{\infty}\frac{F_r(\tau)}{r(\tau)}e^{-i\omega(\tau + r/c)}\,d\tau$$

Expand with Bessel functions

$$P_D(x,\omega) \approx \frac{ik e^{-i\omega R_0/c}}{4\pi R_0}\left\{\int_{-\infty}^{\infty}F(\tau)\cos(\theta)\cos(\gamma)\,e^{ikR_1\sin(\theta)\cos(\Omega\tau-\varphi)}e^{-i\omega\tau}\,d\tau + \int_{-\infty}^{\infty}F(\tau)\sin(\theta)\sin(\gamma)\sin(\Omega\tau-\varphi)\,e^{ikR_1\sin(\theta)\cos(\Omega\tau-\varphi)}e^{-i\omega\tau}\,d\tau\right\}$$

where:

$$P_D(x,\omega) \approx \frac{ik e^{-i\omega R_0/c}}{4\pi R_0}\sum_{n=-\infty}^{n=\infty} i^n J_n(kR_1\sin(\theta))\,e^{-in\varphi}\,\hat{F}(\omega - n\Omega)\left[-\frac{n}{kR_1}\sin(\gamma) + \cos(\theta)\cos(\gamma)\right]$$

Supposing that the force acting on the radial segment is periodic with the fundamental period of rotation $2\pi/\Omega$

The force can be written as a fourier series:

$$F(t) = \frac{1}{2\pi}\int_{-\infty}^{\infty} \hat{F}(\omega) e^{-i\omega t} d\omega = \sum_{s=-\infty}^{\infty} F_s e^{-is\Omega t} \quad \text{with:} \quad F_s = \frac{\Omega}{2\pi}\int_0^{2\pi/\Omega} F(t) e^{is\Omega t}$$

Discrete force spectrum:

$$\hat{F}(\omega) = \sum_{s=-\infty}^{\infty} F_s\, \delta(\omega - s\Omega) \quad \Big\} \text{ Substituting into } P_D(x,\omega)$$

$$P_D(\boldsymbol{x},\omega) \approx \frac{ike^{-i\omega R_0/c}}{4\pi R_0} \sum_{n=-\infty}^{n=\infty} J_n(kR_1 \sin(\theta)) e^{-in(\varphi - \frac{\pi}{2})} \sum_{s=-\infty}^{\infty} F_s \delta(\omega - (s+n)\Omega) \left[-\frac{n}{kR_1}\sin(\gamma) + \cos(\theta)\cos(\gamma)\right]$$

Far field is necessarily discrete with fundamental frequency Ω

$$P_D(x,\omega) = \sum_{N=-\infty}^{\infty} P_N(x)\, \delta(\omega - N\Omega) \qquad s+n = N$$

Obtaining:

$$P_N(x) \approx \frac{iN\Omega e^{-iN\Omega R_0/c}}{4\pi c R_0} \sum_{s=-\infty}^{\infty} F_s e^{-i(N-s)(\varphi - \frac{\pi}{2})} J_{N-s}(N\Omega R_1 \sin(\theta)/c) \left[-\frac{N-s}{N\Omega R_1/c}\sin(\gamma) + \cos(\theta)\cos(\gamma)\right]$$

Discrete noise expectrum: $\quad M = \frac{\Omega R_1}{c}$

$$P_N(x) \approx \frac{iN\Omega e^{-iN\Omega R_0/c}}{4\pi c R_0} \sum_{s=-\infty}^{\infty} F_s e^{-i(N-s)(\varphi - \frac{\pi}{2})} J_{N-s}(NM \sin(\theta)) \left[-\frac{N-s}{NM}\sin(\gamma) + \cos(\theta)\cos(\gamma)\right]$$

\# blades

B equally spaced blades: $e^{-i(N-s)\varphi} \longrightarrow e^{-i(mB-s)(\varphi - \frac{2\pi j}{B})}$ interference function $N = mB$

$$P_{mB}(x) \approx \frac{imB\Omega e^{-imB\Omega R_0/c}}{4\pi c R_0} \sum_{s=-\infty}^{\infty} F_s e^{-i(mB-s)(\varphi - \frac{\pi}{2})} J_{N-s}(mBM \sin(\theta)) \left[-\frac{mB-s}{mBM}\sin(\gamma) + \cos(\theta)\cos(\gamma)\right]$$

$$P_{mB}(x) \approx \frac{imB^2\Omega}{4\pi c R_0} \sum_{s=-\infty}^{\infty} F_s e^{-i(mB-s)\frac{\pi}{2}} e^{i(mB-s)[\varphi - \Omega_s R_0/c]} J_{mB-s}(mBM\sin(\theta)) \left[-\frac{mB-s}{mB}\cdot\frac{\sin(\gamma)}{M} + \cos(\theta)\cos(\gamma)\right] \qquad \Omega_s = \frac{mB\Omega}{mB-s}$$

Properties

1. Periodic blade loading generates discrete-frequency noise at the Blade Passing Frequency $B\Omega/2\pi$ and harmonics.
2. Each tone is the result of the sum of infinite free-field radiation modes (s)
3. The magnitude of each mode is proportional to the blade loading harmonics F_s weighted by Bessel function as a result of Doppler
4. Each mode rotates with equivalent phase speed Ω_s when $s \neq mB$ the mode is an effectively spinning mode which gives zero contribution on the axis
5. The special case $s = mB$ corresponds to the symmetric mode, most efficient one directly related to the J_0 factor. Radiation along the axis.
6. The mode $s = 0$ corresponds to steady contribution of force. Contribution to thrust of propeller. Contribution is smaller than the one from higher blade loading harmonics in non-uniformities of forces.
7. The rotor-locked noise has a zero contribution along the rotor axis at an angle such that $\cos(\theta) = \frac{\tan(\gamma)}{M}$ located in the front of the rotor. If a noise is measured along the axis, harmonic loadings are present.

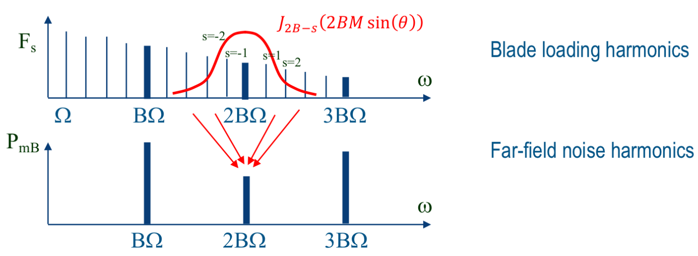

NOISE FROM A ROTOR IN THE WAKE OF A STATOR

A stator of V vanes generates wakes chopped by B-bladed rotor

The loading harmonics acting on the rotor are multiples of the number of vanes (sV)

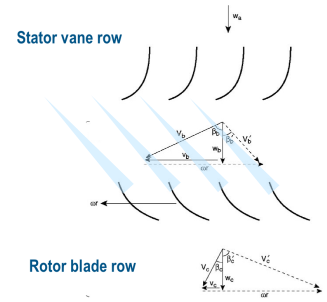

$$P_{mB}(x) \approx \frac{imB^2\Omega}{4\pi c R_0} \sum_{s=-\infty}^{\infty} F_s e^{-i(mB-sV)\frac{\pi}{2}} \; e^{i(mB-sV)[\varphi-\Omega_{sV}R_0/c]} \; J_{mB-sV}(mBM\sin(\theta))\left[-\frac{mB-sV}{mB}\frac{\sin(\gamma)}{M}+\cos(\theta)\cos(\gamma)\right] \quad \Omega_{sV}=\frac{mB\Omega}{mB-sV}$$

NOISE FROM A STATOR IN THE WAKE OF A ROTOR

A rotor of B blades generates wakes impinging on a V-vaned stator.

The loading harmonics acting on the rotor are multiples of the number of vanes (sV)

The force do not rotate; the first vane angle is α_0

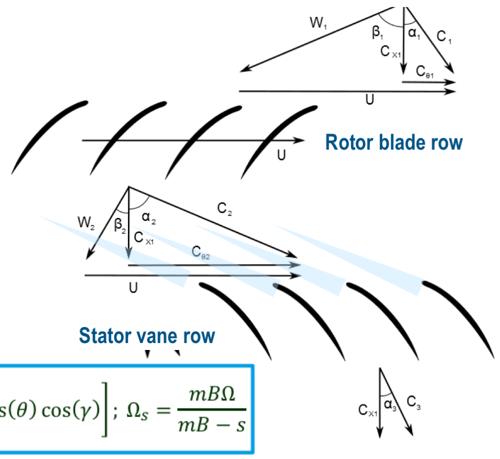

$$P_{mB}(x) \approx \frac{imBV\Omega}{4\pi c R_0} F_{mB} \sum_{s=-\infty}^{\infty} e^{-i(mB-s)(\frac{\pi}{2}+\alpha_0)} \; e^{i(mB-s)[\varphi-\Omega_{sV}R_0/c]} \; J_{mB-sV}(mBM\sin(\theta))\left[+\frac{mB-sV}{mB}\frac{\sin(\gamma)}{M}+\cos(\theta)\cos(\gamma)\right]; \; \Omega_s=\frac{mB\Omega}{mB-s}$$

PROPELLER NOISE

SPECTRA AND SOURCES OF NOISE

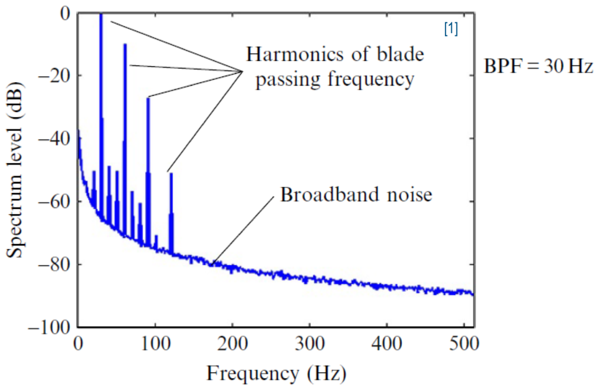

Tonal noise:

- Loading noise
- Thickness noise

Broadband noise:

- Turbulent boundary layer trailing edge noise

Blade Passing Frequency

$BPF = \frac{B}{T_p} = f B$

T_p: period of one revolution

B: # blades $\quad f$: rotational frequency

$$\rho'(x,t)\,c_0^2 = \frac{\partial^2}{\partial x_i \partial x_j}\int_{V_0}\left[\frac{T_{ij}}{4\pi r\,|1-M_r|}\right]_{\tau=\tau^*} dV(z) \; \underbrace{- \frac{\partial}{\partial x_i}\int_{S_0}\left[\frac{P_{ij}\cdot n_j}{4\pi r\,|1-M_r|}\right]_{\tau=\tau^*}}_{\text{Loading noise: Steady and unsteady pressure contribution on the surface}} \; + \; \underbrace{\frac{\partial}{\partial t}\int_{S_0}\left[\frac{\rho_0 \cdot V_j\, n_j}{4\pi r\,|1-M_r|}\right]_{\tau=\tau^*}}_{\text{Thickness noise: Contribution from the blade surface motion}}$$

(M>0.7) important!

BROADBAND NOISE – FREQUENCY DOMAIN:

TRAILING EDGE NOISE

Blade section of chord "c" and a span length "L" with mean flow in the x direction. Far field noise due to trailing edge noise

$$S_{pp}^{TE}(x,\omega) = \left(\frac{\bar{k}z}{2\pi\sigma^2}\right)^2 2c \int_{-\infty}^{\infty} \Phi_{pp}\left(\frac{\omega}{U_c}, k_y\right) \frac{\sin^2\left[\frac{L}{c}\left(\bar{k}_y - \frac{\bar{k}z}{\sigma}\right)\right]}{\left(\bar{k}_y - \frac{\bar{k}z}{\sigma}\right)^2} \cdot \left| I^{TE}\left(\frac{\bar{k}}{U_c}, \bar{k}_y\right)\right|^2 d\bar{k}_y$$

$\bar{k} = \frac{\omega c}{2a_0}$ non dimensional acoustic wave number

$\sigma = \sqrt{x^2 + \beta^2(y^2+z^2)}$ P-G transformed distance from trailing edge

$\beta^2 = \sqrt{1-M^2}$

Φ_{pp} wall pressure wave number freq. espectrum

U_c boundary layer eddy convective velocity

$\bar{k}_y = \frac{k_y c}{2}$

I^{TE}: radiation integral function

Radiation integral function is the sum of:

$$I^{TE} = I_1^{TE} + I_2^{TE}$$

I_2^{TE} → Accounts for the wave back reflection at the leading edge.

I_1^{TE} → derived from semi-infinite flat plate

$$I_1^{TE} = \frac{ie^{2iC}}{C}\left\{(1+i)e^{-2iC}\sqrt{\frac{B}{B-C}}E^*(2B-2C) - (1+i)E^*(2B) + 1\right\}$$

$$I_2^{TE} = H\{e^{4i\kappa}[1-(1+i)E^*(4\bar{\kappa})]\}^{\varepsilon} + H[-e^{2i\Theta} + i(\Theta + \bar{k}_x + M\bar{\mu} - \bar{k})G]$$

$\bar{k}_x = \frac{k_x c}{2}$ nondimensional wave number streamwise.

$M = \frac{U_0}{a_0}$ average mach number

$\bar{\mu} = \frac{\omega c}{(2U_0\beta^2)}$

Rest is more equations...

E^* Fresnel integral

The wall pressure wave number is given by:

$$\Phi_{pp}(\omega/U_c, k_y) = \frac{\phi_{pp}(\omega) l_y(\omega, k_y)}{\pi}$$

where:

$$l_y(\omega, k_y) = \frac{bU_c}{\omega}, \text{ b calibration constant}$$

$$\phi_{pp}\left(\frac{\omega\delta^*}{U_0}\right) = \frac{(\tau_w^2\delta^*/U_0)0.78(1.8\Pi\beta_c + 6)\left(\frac{\omega\delta^*}{U_0}\right)^2}{\left[\left(\frac{\omega\delta^*}{U_0}\right)^{0.75} + 0{,}105\right]^{3.7} + \left[3.76Re_T^{-0.57}\left(\frac{\omega\delta^*}{U_0}\right)\right]^7}$$

δ^* boundary layer displacement thickness

τ_w wall shear stress.

LEADING EDGE NOISE:

Far field noise due to impinging turbulent fluctuations.

- $$S_{pp}^{LE}(\boldsymbol{x},\omega) = \left(\frac{\rho_0\bar{k}z}{\sigma^2}\right)^2 \pi U_0 \frac{L}{2}\int_{-\infty}^{\infty}\Phi_{\omega\omega}\left(\frac{\omega}{U_0}, k_y\right)\frac{\sin^2\left[\frac{L}{2}\left(\frac{ky}{\sigma} - ky\right)\right]}{\frac{\pi}{2}\left(\frac{ky}{\sigma} - k_y\right)^2 \left|I^{LE}\left(x, \frac{\omega}{U_0}, k_y\right)\right|^2} dk_y$$

I^{LE} takes into account both the leading edge contribution and the backscattering of TE.

$$I_1^{TE} = -\frac{1}{\pi}\sqrt{\frac{2}{(\bar{k}_x + \beta^2\bar{\kappa})\Theta^-}}e^{-i\Theta}E(2\Theta)$$

$$I_2^{TE} = \frac{e^{-i\Theta}}{\pi\Theta\sqrt{2\pi(\bar{k}_x + \beta^2\bar{\kappa})}}\left\{i(1-e^{2i\Theta^-}) - (1+i)\left[E(4\bar{\kappa}) - e^{2i\Theta^-}\sqrt{\frac{2\bar{\kappa}}{\Theta^+}}E(2\Theta^+)\right]\right\}$$

Φ_{ww} can be related to the velocity power espectral density $\phi_{ww}(\omega)$ and spanwise correlation length $l_y(\omega, k_y)$

$$\Phi_{\omega\omega}\left(\frac{\omega}{U_0}, k_y\right) = \frac{U_0 \phi_{\omega\omega}(\omega) l_y(\omega, k_y)}{\pi}$$

Assuming frozen convected homogeneous isotropic turbulence ($\omega = k_x U_0$)

$$\phi_{\omega\omega}(k_x) = \frac{\overline{u}'^2 L_t}{2\pi U_0} \frac{1+\frac{8}{3}(k_x+k_e)^2}{\left[1+\left(\frac{k_x}{k_e}\right)^2\right]^{\frac{11}{6}}} \qquad l_y(k_x) = \left[\frac{\Gamma\left(\frac{1}{3}\right)}{\Gamma\left(\frac{5}{6}\right)}\right]^2 \frac{\left(\frac{k_x}{k_e}\right)^2}{[3+8(k_x+k_e)^2]\sqrt{1+(k_x+k_e)^2}}$$

$L_t = 0.4\, k^{1.5}/\varepsilon$ → k is the turbulent kinetic energy and ε is the dissipation rate.

IMPLEMENTING A ROTATING REFERENCE SYSTEM

Apply a frequency shift correction to each section to account for the Doppler effect

$$\frac{\omega_e(\psi)}{\omega} = 1 + \frac{M_t \cdot \sin\theta \, \sin\psi}{\sqrt{1 - M_z^2 \sin^2(\theta)}}$$

M_z and M_t : axial and tip mach numbers

COMPARISON WITH EXPERIMENTS

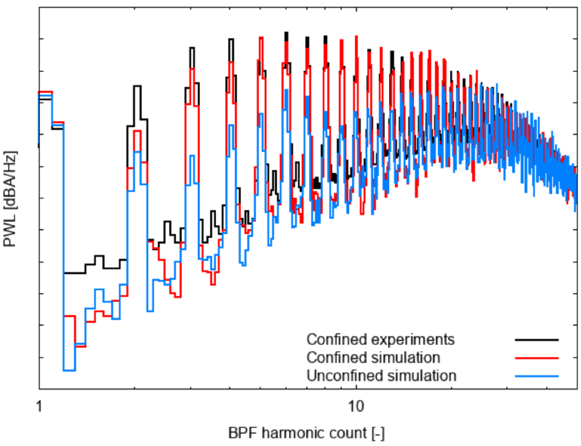

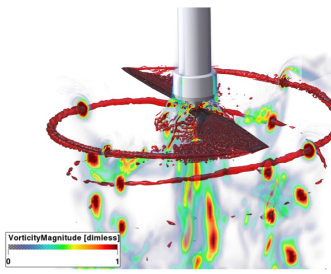

Unconfined

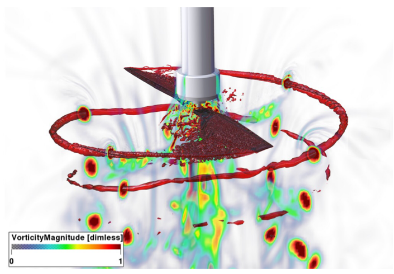

Confined

increases the peaks mostly.

Airfoil Self Noise

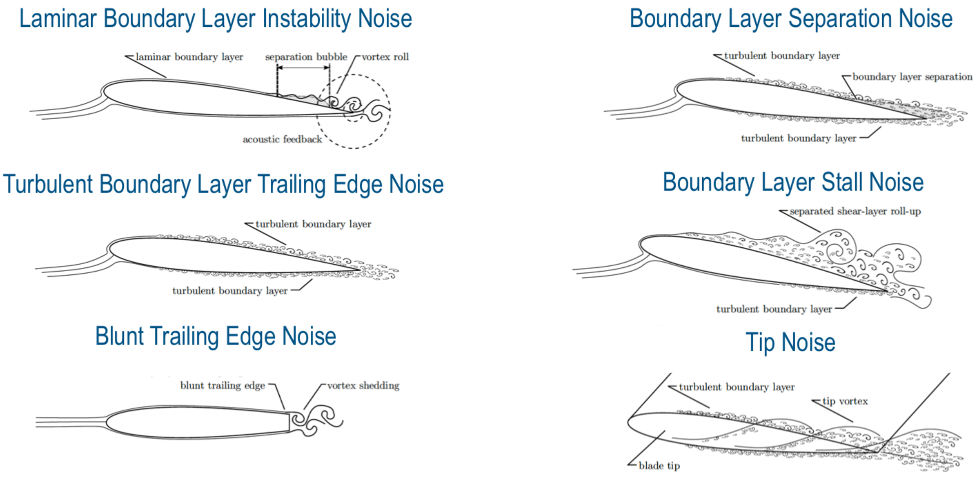

Laminar Boundary Layer Instability Noise

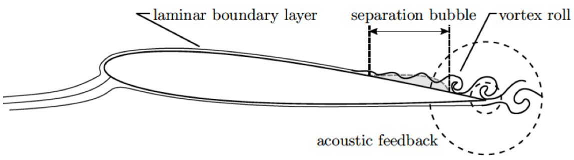

- ==Tonal noise==
- Low Reynolds number ($50\,000 < Re < 500\,000$)
- Small perturbation in laminar b-l are amplified coherently over a laminar separation bubble or separated shear layer.
- These amplified instability waves pass the trailing edge and scatter sound
- Propagate upstream and they trigger new instability waves.

Turbulent Boundary Layer Trailing Edge Noise

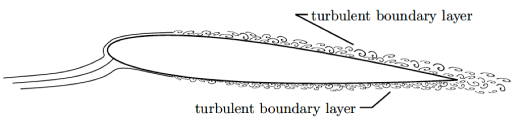

- ==Broadband Noise==
- Characteristics of $Re > 500\,000$
- Random organization
- Different pressure forces between suction and pressure sides leads to scattering

Blunt Trailing Edge Noise

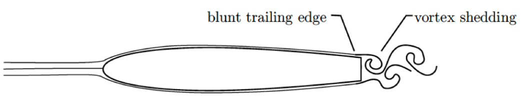

- For blunt trailing edge ==Tonal noise==
- Vortex shedding happens, vortex by roll up process
- This vortex shedding is restricted to a narrow band of frequency.
- Dominate over turbulent boundary layer TE noise

Separation and Stall Noise

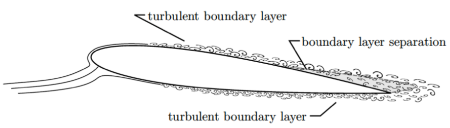

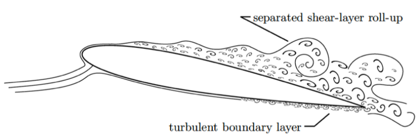

- At high angles of attack the flow can separate on the suction side and generate shedding of vortices ==Tonal Noise==
- Deep stall happens at high angles of attack.
- Large scale structures, low frequency noise

Tip Noise

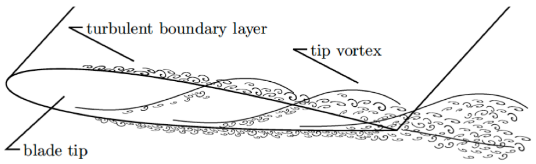

- Only encountered on a finite wing
- Related to the tip vortices
- Generate noise, unsteady

Trailing Edge Noise

Effect of Solid Boundary

Lighthill: noise generated by turbulence in an unbounded medium.

$$I \propto \rho u_\infty^3 M_0^5 \frac{\delta^2}{R^2}$$

ρ density of the medium
M_0 Mach number
δ length scale of the turbulent flow
R distance from the observer
L span of the surface
c chord of the surface
He Helmholtz number
λ_a acoustic wavelength
k acoustic wavenumber
q_∞ dynamic pressure

Curle: influence of solid boundary upon the radiation of sound.

$$I \propto \rho u_\infty^3 M_0^3 \frac{c^2}{R^2} \frac{L}{c} \qquad \propto u_\infty^6 \qquad \propto q_\infty^2$$

stronger sound emission at low mach numbers in presence of a surface

If $He = kc = 2\pi c/\lambda_a \ll 1$ the source can be treated as point source validity ↓

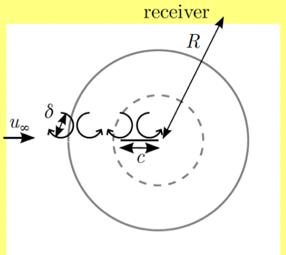

Compact surface

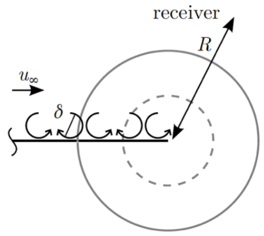

Non-compact surface

- If the train of eddies has wavelength $\lambda = 2\delta$ with δ the length scale of turbulence.
- If the train of eddies convects at velocity U_∞ and angular frequency $\omega = \frac{2\pi U_\infty}{\lambda}$

Non Compact Surface

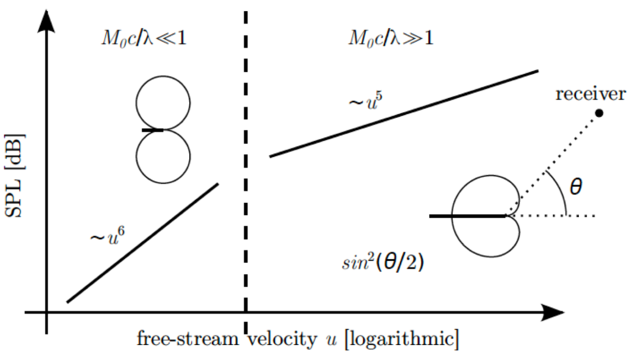

$$I \propto \rho u_\infty^3 M_0^2 \frac{\delta^2}{R^2} \cdot \frac{L}{\delta} \sin^2(\theta/2)$$

for non-compact surfaces sound radiation is directed toward the upstream direction.

Effect of Airfoil Geometry

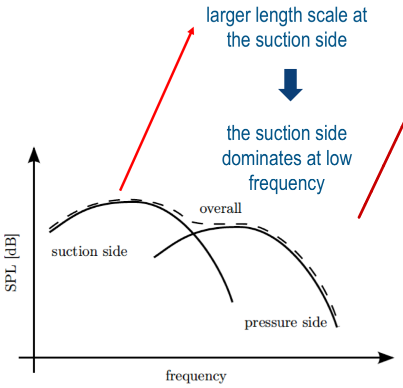

- If $T/\delta^* < 3.3$, the airfoil is considered sharp where T is the TE thickness and δ^* is the displacement thickness at TE.
  - At attached flows, radiated noise is broadband.

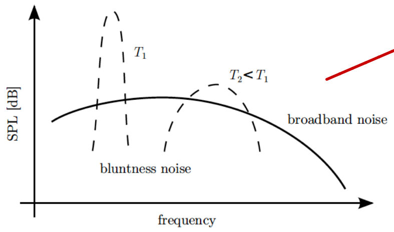

- If $T/\delta^* > 3.3$, vortex shedding linked to tonal noise occurs.

Diffraction Theory

Incident Gust Description

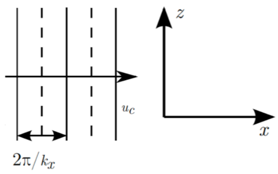

2D pressure gust

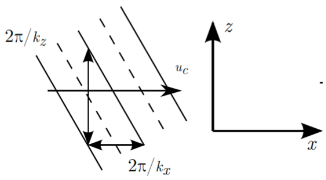

3D pressure gust

Assume frozen turbulence:

If the airfoil is thin and the camber small ($k_y = 0$), the surface pressure expressed as:

$$p(t,x,y,z) = p(t,x,0,z) = P_0 e^{i(\omega t - k_x x - k_z z)}$$

$$P(t,x,0,z) = P_0 e^{i(\underline{\omega/k_x t} - x - k_z/k_x z)k_x}$$

for a given location z the phase is constant.

In a turbulent b-l. convection is mainly directed in streamwise direction.

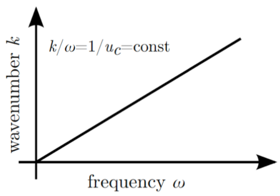

Constant convective velocity

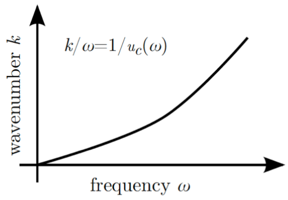

Varying convective velocity

Solution of the Semi-Infinite Half Plane

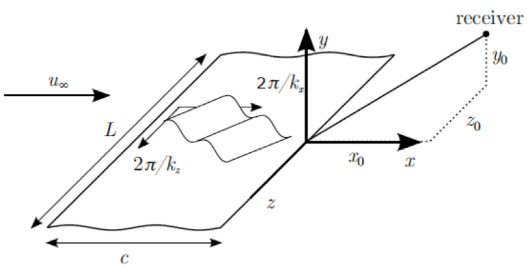

Ignoring equations:

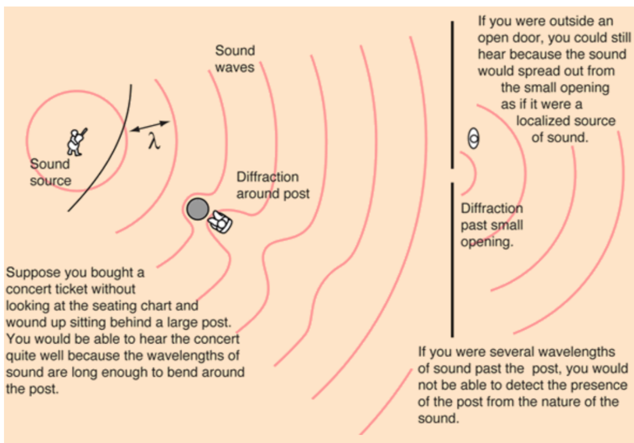

The auto-spectral density of the far-field acoustic pressure is:

$$\Phi_{aa} = \left(\frac{k c y_0}{4\pi S_0^2}\right)^2 2\pi L \left|\underbrace{\mathcal{L}_1\left(\frac{\omega}{u_c}, 0\right)}_{\text{acoustic transfer function}}\right|^2 \underbrace{\Pi_0(\omega, 0)}_{\text{wavenumber freq. spectrum}}$$

In 3D, $k_z \neq 0 \rightarrow \left(k \cdot \frac{z_0}{S_0}\right)$ replaced

$$\mathcal{L} = \mathcal{L}_1 + \mathcal{L}_2$$

$\mathcal{L}_1$: direct scattering

$\mathcal{L}_2$: back scattering

Laminar Boundary Layer Instability Noise (in detail)

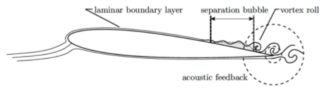

Ladder-type spectrum: the primary tone constitutes the ladder

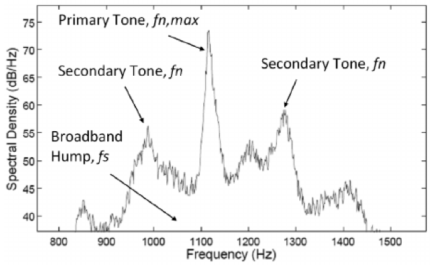

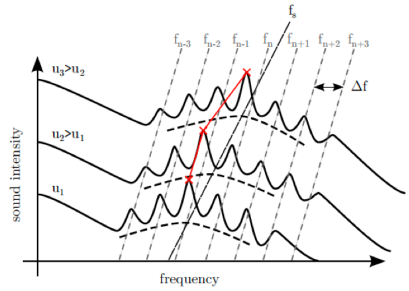

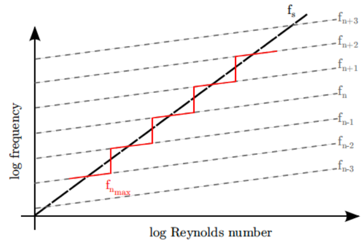

Frequency jump as function of Re

Ladder structure: caused by the frequency lag between the scattering of the boundary layer instability noise and the discrete noise produced by a aeroacoustic feedback loop. } superposition of tones at frequencies f_n and broadband energy content centred at a frequency f_s.

Instability Concepts TAM

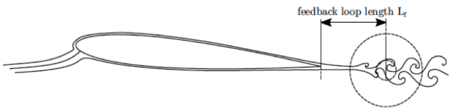

Wake instability concept (Tam 1974)

Hypothesis:

- Total change of phase over feedback loop is equal to a integer multiple of 2π
- The length of loop is L_f
- Constant convective velocity for the instability waves.

FEEDBACK

Phase condition for feedback loop:

$$\frac{2\pi L_f}{\lambda} = \frac{2\pi L_f f}{u_c} \quad \text{change in phase of instability}$$

$$\frac{2\pi L_f}{\lambda_a} = \frac{2\pi L_f f}{c_0} \quad \text{change in phase of upstream travelling acoustic wave}$$

$$2\pi f_n L_f \left(\underbrace{\frac{1}{u_c} + \frac{1}{c_0}}_{} \right) = 2\pi n$$

varies with airfoil, free stream velocity and angle of attack

$$St_{f_n} = \frac{f_n L_f}{u_\infty} = \frac{n}{u_\infty/u_c + u_\infty/c_0}$$

Instability Concepts ARDEY

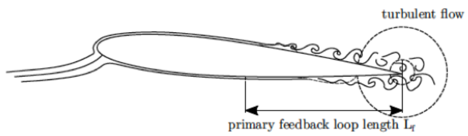

Laminar Boundary Layer Instability Concept (Arbey et al. 1983)

- Acoustic pressure at the frequency of the instability waves is proportional to the wall pressure fluctuations near the trailing edge

Best fit at phase diff of π.

- Reason: scattering of surface pressure perturbations induced by instability waves, developing in the b-l and amplified through a separation bubble upstream of TE.

$$St_{f_n} = \frac{f_n L_f}{u_\infty} = \frac{\left(n + \frac{1}{2}\right) n}{u_\infty/u_c + u_\infty/(c_0 - u_\infty)}$$

phase diff of π due to diffraction stability waves at TE Kutta

Instability Concepts — Desquenses

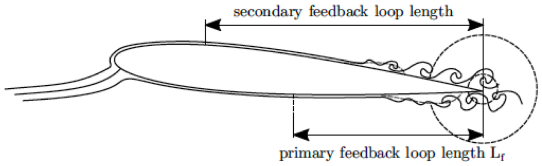

The modulation of the primary tone may be cause by a secondary feedback loop that modulates the main feedback loop. Might explain the presence of multiple tones.

Blunt Trailing Edge Noise (in detail)

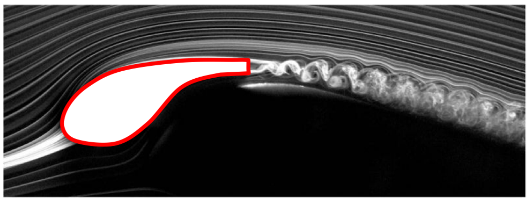

$$\frac{t_{TE}}{\delta^*_{TE}} > 3.3$$

t_{TE} → airfoil thickness at TE

δ^*_{TE} → b-l displacement thickness at trailing edge

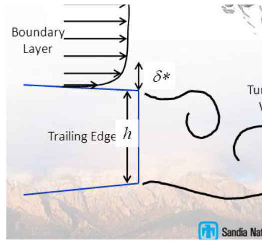

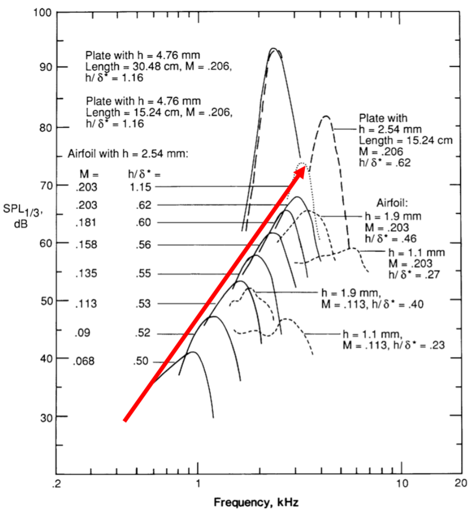

- As the ratio increases the band-width of the noise decreases
- The tonal noise contribution rises
- More noise is generated.

Hypothesis

- Only parallel gusts contribute to radiated sound. The vortex shedding leads to high correlation of upwash velocity.

$$\Phi_{aa}(\omega,\mathbf{x}_0) = \left(\frac{\rho_0 k c y_0 u_\infty}{2S_0^2}\right)^2 \frac{L}{2}\underbrace{\Phi_{vv}(\omega)}_{\text{Autospectrum of the upwash velocity}}\overbrace{l_z(\omega)}^{\text{Spanwise correlation length}}\underbrace{|\mathcal{L}_{VK}|^2}_{\text{Normalized radiation integral}}$$

Jet Noise

The engine jet is one of the biggest contributions to noise on aircraft.

Subsonic

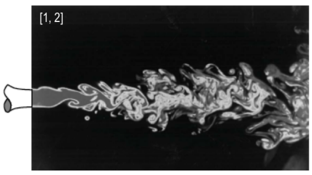

Supersonic

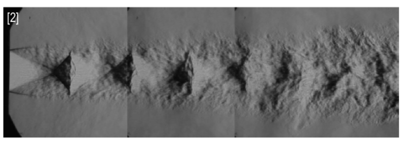

$$\square^2 p' = \cancel{\square} + \cancel{\square} + \boxed{T_{ij}}$$

- Viscous ← from laminar to turbulent, viscous forces are more relevant
- Conv $(p - \rho c)\delta$
- Non-linear

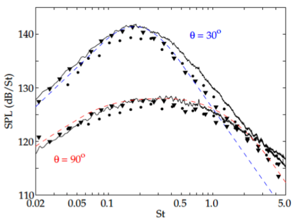

Mixing noise

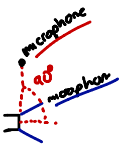

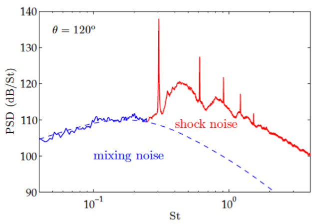

Mixing noise and shock noise

SUBSONIC JET

Dependence on Re:

[1]

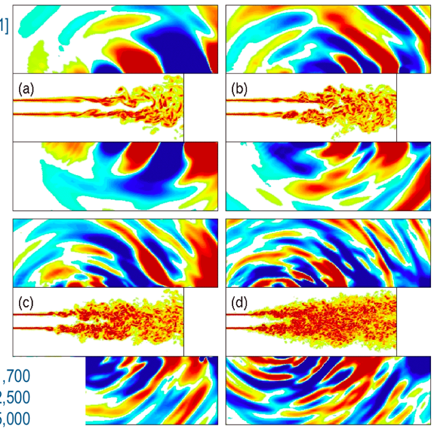

(a) M = 0.9; Re_D = 1,700
(b) M = 0.9; Re_D = 2,500
(c) M = 0.9; Re_D = 5,000
(d) M = 0.9; Re_D = 400,000

SAME!

Re_D = 5,600

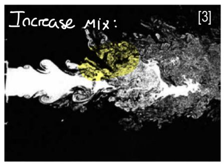

Re_D = 11,000

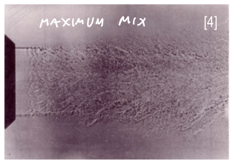

Re_D = 460,000

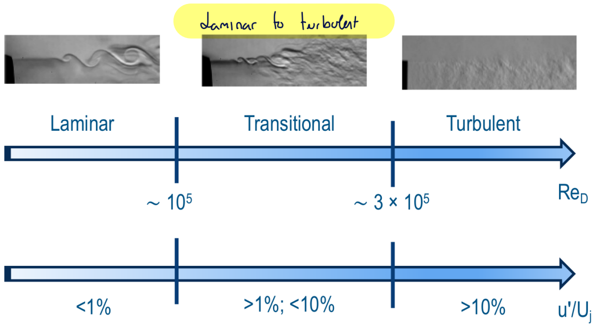

JET FLOW DEVELOPMENT

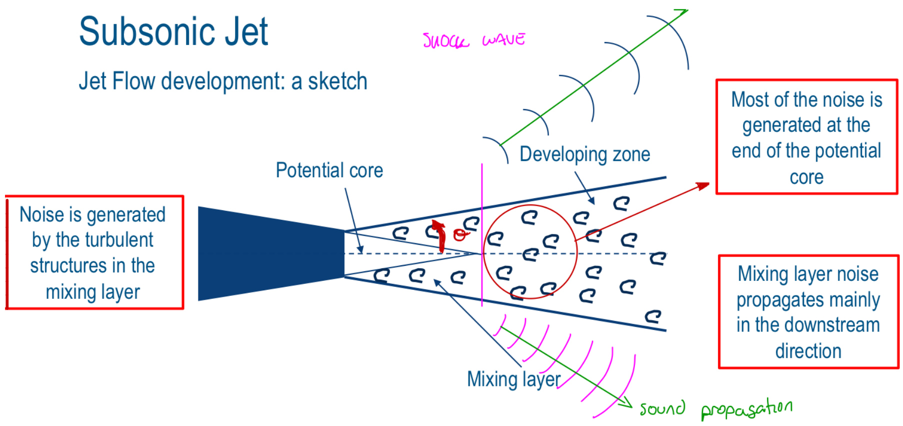

MIXING LAYER NOISE: DIRECTIVITY

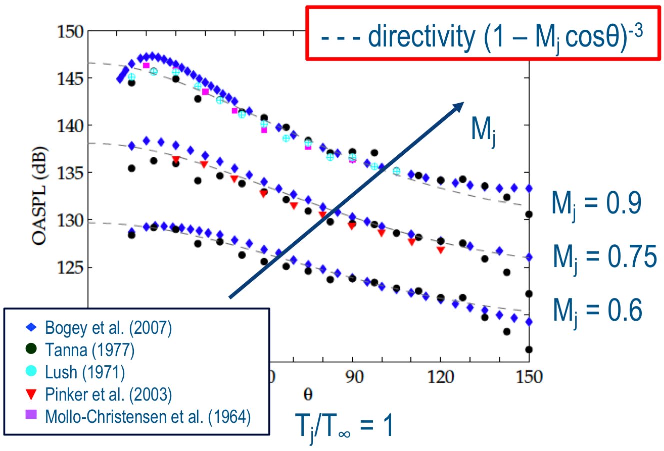

M_j = 0.98
M_j = 0.9
M_j = 0.75
M_j = 0.6

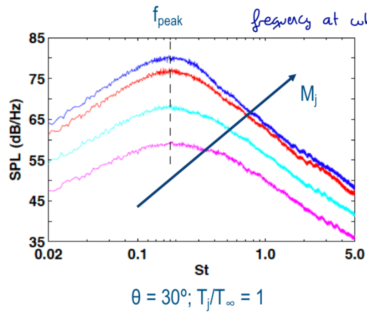

f_{peak} frequency at which you have most of the noise. ≠ M

f_{peak} scales with $St = fD/U_j$

$SPL \propto (U_j/c_\infty)^{11}$

11 power

Low Mach, TE noise, more relevant

higher Mach, Jet noise more relevant

LIGHTHILL'S ACOUSTIC ANALOGY

$$T_{ij} = \underbrace{\rho u_i u_j}_{\text{sound generated by unsteady convection of flow}} + \overbrace{(p - \rho c_\infty^2)}^{\text{Non-linear acoustic generation}}\delta_{ij} - \underbrace{\tau_{ij}}_{\text{sound generated by viscous effects}}$$

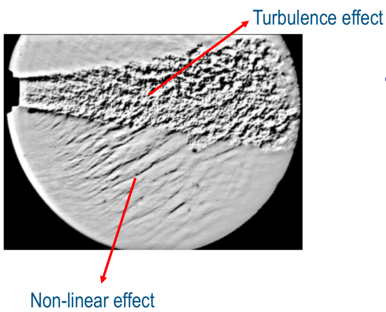

$$p(x,t) = \frac{1}{4\pi c_\infty^2}\int_V \frac{\partial^2 T_{ij}}{\partial y_i \partial y_j}\underbrace{\left(y, t - \frac{r}{c_\infty}\right)}_{\text{retarded time}}\frac{1}{r}\,dy$$

Assuming that the source moves at velocity U

$$M = \frac{U}{c_\infty}$$

We define a moving coordinate system such that the source emits when crossing y at time τ:

$$\eta = y - c_\infty M\left(t - \frac{r}{c_\infty}\right) = y - c_\infty M\tau$$

Giving the following equation:

$$\boxed{\rho(\mathbf{x}, t) = \frac{1}{4\pi c_\infty^2}\int_V \frac{\partial^2 T_{ij}}{\partial\eta_i\partial\eta_j}\left(\boldsymbol{\eta}, t - \frac{r}{c_\infty}\right)\frac{1}{|\mathbf{r} - \mathbf{M}(\mathbf{x} - \mathbf{y})|}\, d\boldsymbol{\eta}}$$

The source term is equal to the double divergence, that, neglecting the retarded time, in the far field is zero.

if $|x| \gg |y|$

$$\boxed{\rho(\mathbf{x}, t) \approx \frac{1}{4\pi c_\infty^4}\frac{x_i x_j}{x^3}\int_V \frac{\partial^2 T_{ij}(\mathbf{y}, \tau)}{\partial\tau^2}\, d\mathbf{y}}$$

$$\frac{x_i x_j}{x^2} T_{ij} = T_{xx}$$

$$\boxed{\rho(\mathbf{x}, t) \approx \frac{1}{4\pi c_\infty^4 x}\int_V \frac{\partial^2 T_{xx}(\mathbf{y}, \tau)}{\partial\tau^2}\, d\mathbf{y}}$$

The contribution to the far field noise involves only the components aligned in the direction from x to y and its amplitude is proportional to the second time derivative of T_{ij} at emission.

All the sources radiate regardless of their position with respect to the flow boundaries

Ratio of kinetic energy escaping as sound:

$$\frac{\dfrac{\partial^2 T_{ij}}{\partial y_i \partial y_j}}{\dfrac{\partial^2 T_{ij}}{\partial\tau^2}\dfrac{\partial\tau}{\partial y_i}\dfrac{\partial\tau}{\partial y_j}} = \mathcal{O}\left(\frac{u_0^2}{c_\infty^2}\right)$$

P_a acoustic power

$$\boxed{P_a = \frac{K\rho_j^2 A_j U_j^8}{\rho_\infty c_\infty^5}} \xrightarrow{P_j = \rho_j A_j U_j^3} \boxed{\frac{P_a}{P_j} = K\frac{\rho_j}{\rho_\infty}\left(\frac{U_j}{c_\infty}\right)^5}$$

Only a small fraction of energy scapes as noise.

Simplification

$$T_{ij} = \rho u_i u_j + (p - c_\infty^2)\delta_{ij} - \tau_{ij}$$

$\downarrow$ High Re_D

$$T_{ij} \approx \rho u_i u_j + (p - \rho c_\infty)\delta_{ij}$$

$\downarrow$ Perfect gas: $p' = c_\infty^2 + \dfrac{p_\infty}{c_v}s'$

$$T_{ij} \approx \rho u_i u_j$$ isotropic flows

$\downarrow$ Low M

Non linear part is lost!

$$T_{ij} \approx \rho_\infty \underbrace{u_i u_j}$$

Linear compression part is preserved

Effect of Temperature

Assuming a high Re number

$$\frac{\text{Dipole}}{\text{Quadrupole}} = 1.6\,\frac{T_j}{T_\infty}\cdot\frac{c_\infty}{U_j}$$

$\downarrow$ Non isothermal jet dipole sources become relevant.

Dependence is M^6

Effect of Convection

- Assuming that dominant sources are all convected downstream parallel to the jet axis at a constant convective velocity U_c and Mach M_c
- When source is convected relative to the observer the radiation is directed in the downstream direction.

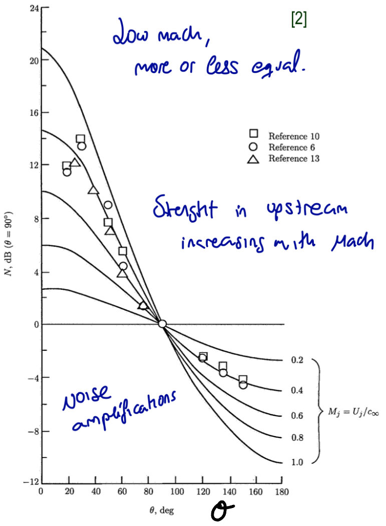

SUPERSONIC JET

SUPERSONIC JET NOISE CAUSED BY INSTABILITY WAVES

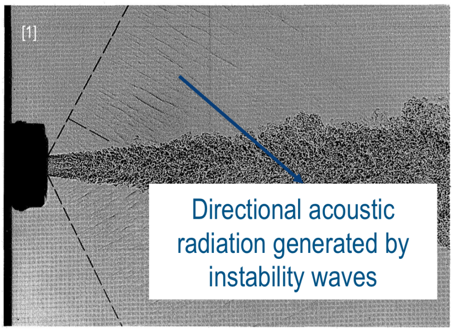

Generated really close to the jet exit

They may be generated by instability waves in the mixing layer.

Has a near field acoustic field, similar and propagates with a velocity smaller than speed of sound.

NOZZLE DESIGN CONDITION NOT SATISFIED:

Turbulent mixing noise + shock associated noise
downstream propagating   upstream propagating

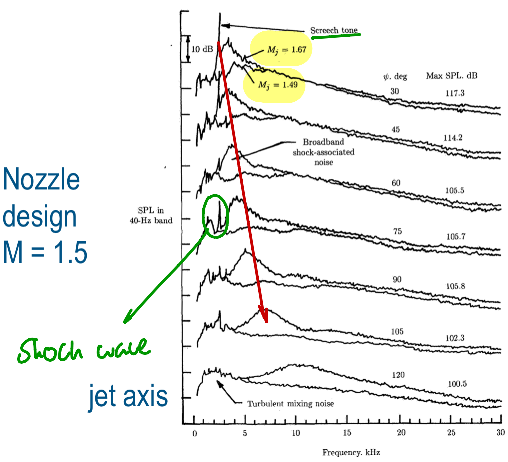

The frequency of the shock associated noise changes with the direction of propagation

The fundamental screech tone has frequency smaller than the broadband contribution.

The screech tone can be seen as lower bound of the broadband associated noise spectrum.

SCREECH TONES: supersonic engine in sub design (propagates upstream)

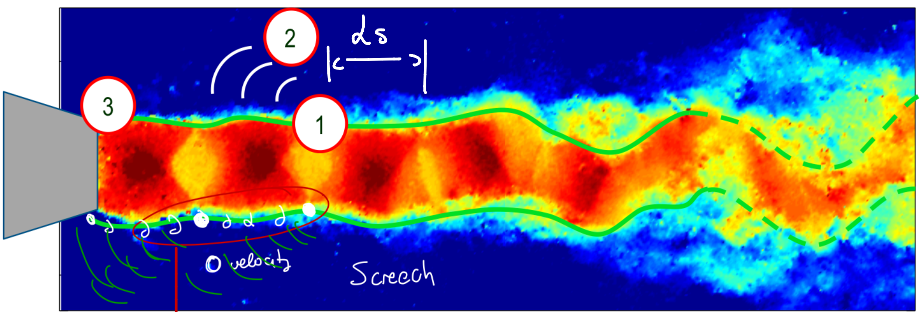

Instabilities and discontinuities create noise

1. Interaction between large vortices in the shear layer and the shock cell which turns into an oscillatory motion
2. Generation of acoustic waves propagating upstream
3. Interaction between acoustic waves and lip produces vortex.

Period of oscillation is equal to the time for a disturbance to travel one shock cell inside the wake + the time to travel upstream.

$$f_s = \frac{U_c}{d_s(1+M_c)}$$

SUBSONIC JET : JET NOISE MODELLING

RANS using $k-\varepsilon$ for turbulence intensity and length scale.

Approaches for modelling: Lighthill's, Tam, Auriant.

LIGHTHILLS ANALOGY:

$$\boxed{\rho(\mathbf{x},t) \approx \frac{1}{4\pi c_\infty^4 x}\int_V \frac{\partial^2 T_{xx}(\mathbf{y},\tau)}{\partial \tau^2}\,d\mathbf{y}}$$

$$\tau = t - \frac{r}{c_\infty}$$

The far-field spectra for the intensity of the sound field are related to the fourier transform of the autocorrelation function of the far-field pressure.

$$S(\mathbf{x},\omega) = \frac{1}{2\pi}\int_{-\infty}^{+\infty} \frac{\langle p(\mathbf{x},t)p(\mathbf{x},t+\tau)\rangle}{\rho_\infty c_\infty} e^{i\omega\tau} d\tau$$

$$S(\mathbf{x},\omega) = \frac{1}{32\pi^3\rho_\infty c_\infty^5 x^2}\int_{-\infty}^{+\infty}\int_{V(\mathbf{y}_1)}\int_{V(\mathbf{y}_2)} \left\langle \frac{\partial^2 T_{xx}(\mathbf{y}_1,t_1)}{\partial t^2}\frac{\partial^2 T_{xx}(\mathbf{y}_2,t_2)}{\partial t^2}\right\rangle e^{i\omega\tau} d\mathbf{y}_1 d\mathbf{y}_2 d\tau$$

Turbolent statistics are stationary.

$$S(\mathbf{x},\omega) = \frac{1}{32\pi^3\rho_\infty c_\infty^5 x^2}\int_{-\infty}^{+\infty}\int_{V(\mathbf{y}_1)}\int_{V(\mathbf{y}_2)} \frac{\partial^4}{\partial \tau^4}\langle T_{xx}(\mathbf{y}_1,t)T_{xx}(\mathbf{y}_2,\tau_0)\rangle e^{i\omega\tau} d\mathbf{y}_1 d\mathbf{y}_2 d\tau$$

$R_f(y_1,\eta,\tau) = \langle T_{xx}(y_1,t)T_{xx}(y_2,t+\tau)\rangle$

$\eta = y_2 - y_1$

+ source convection a moving reference frame

$\zeta = \eta - M_c c_\infty \cdot \tau$

$$S(\mathbf{x},\omega) = \frac{\omega^4}{32\pi^3\rho_\infty c_\infty^5 x^2}\int_{-\infty}^{+\infty}\int_{V(\mathbf{y}_1)}\int_{V(\boldsymbol{\eta})} e^{i\omega\left[(1-M_c\cos\theta)\tau - \frac{\mathbf{x}}{x}\cdot\frac{\boldsymbol{\zeta}}{c_\infty}\right]} R_m(\mathbf{y}_1,\boldsymbol{\zeta},\tau)\,d\boldsymbol{\zeta}\,d\mathbf{y}_1 d\tau$$

- Far field noise depends on the source wavenumber frequency spectrum with a wavenumber that gives a sonic velocity in the direction of the far-field and a dopler shifted frequency.

wavenumber-frequency spectrum of turbolence sources is given by

$$H(\mathbf{y}_1,\boldsymbol{\alpha},\omega) = \frac{1}{(2\pi)^4}\int_{V(\zeta)}\int_{-\infty}^{+\infty} e^{i(\omega\tau-\boldsymbol{\alpha}\cdot\boldsymbol{\zeta})} R_m(\mathbf{y}_1,\boldsymbol{\zeta},\tau)\,d\boldsymbol{\zeta}\,d\tau$$

$$\boxed{S(\mathbf{x},\omega) = \frac{\pi\omega^4}{2\rho_\infty c_\infty^5 x^2}\int_{V(\mathbf{y}_1)} H\left[\mathbf{y}_1,\frac{\omega\boldsymbol{x}}{xc_\infty},\omega(1-M_c\cos\theta)\right]d\mathbf{y}_1}$$

$$R_m(y_1,\zeta,\tau) = A^2\rho_0^2 u_0^2 e^{-\frac{|\zeta|^2}{l_0^2}-\omega_0^2\tau^2}$$

magnitude of correlation

velocity scale that characterizes turbolent fluctuations

characteristic length scale.

$\hookrightarrow$ characteristic frequency

$M \ll 1$, compact source

$\alpha l_0 \approx M$ characteristic Mach of turbulence

$$\boxed{H\left[\mathbf{y}_1,\frac{\omega\mathbf{x}}{xc_\infty},\omega(1-M_c\cos\theta)\right] = \frac{A^2}{(2\pi)^4}\rho_0^2 u_0^4\frac{\pi^2 l_0^3}{\omega_0} e^{-\frac{\omega^2(1-M_c\cos\theta)^2}{4\omega_0^4}} e^{-\frac{(\alpha l_0)^2}{4}}}$$

at $\theta = 90°$

$$S(\mathbf{x},\omega) = \frac{A^2}{32\pi\rho_\infty c_\infty^5 x^2}\int_{V(\mathbf{y}_1)} \rho_0^2 u_0^4 l_0^3\, \omega_0^3 \left(\frac{\omega}{\omega_0}\right)^4 e^{-\frac{\omega^2}{4\omega_0^2}} d\mathbf{y}_1$$

If a RANS solution is available is possible to estimate contribution of each elemental volume.

$$\omega_0 = \frac{2\pi}{\tau_0}, \quad \tau_0 = c_\tau \frac{k}{\epsilon}, \quad l_0 = c_l \frac{k^{\frac{3}{2}}}{\epsilon}, \quad u_0 = \sqrt{\frac{2k}{3}}$$

They vary nearly linearly with axial distance

$$dS(\mathbf{x},\omega) = \frac{A^2 c_l^3}{c_\tau^3}\frac{\pi^2}{9\rho_\infty c_\infty^5 x^2}\left[\rho_0^2 k^{\frac{7}{2}} \left(\frac{\omega}{\omega_0}\right)^4 e^{-\frac{\omega^2}{4\omega_0^2}}\right] dV$$

describes how each volume contributes to a range of frequency about the local characteristic frequency

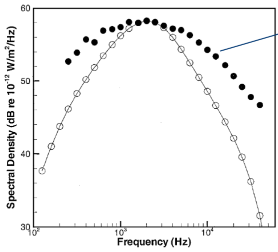

experiments

match peak but not pitch.

Tam and Auriant Method

Lighthill

- Based on full equations of motion
- Source is compact
- Two-point correlation function in a moving reference frame
- Free-space Green's function

Tam and Auriault

- Heuristic argument for the description of the noise sources
- Euler equation for propagation of sound generated
- No assumption on compactness of the noise source
- Two-point correlation in a fixed reference frame
- The Green's function is obtained from the adjoint solution of the lineared Euler equation

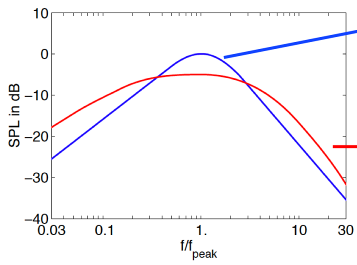

Large scales

Small scales

Small scale turbulence generates local pressure fluctuations proportional to the local turbulent kinetic energy.

$$P_{turb} = \frac{1}{3}\bar{\rho}\langle v^2\rangle = \frac{2}{3}\bar{\rho}k_s \rightarrow \text{kinetic energy of the small scale turbulence per unit mass.}$$

$\langle v^2 \rangle$ → random molecular velocity

Use Euler for propagation.

The equations are rewritten in cylindrical polar coordinates and the assumption of parallel flow is made.

They use adjoint equation to describe the mean flow acoustic iteration effect.

Derivation using adjoint equation in cylindrical coordinates, Greens function, convolution, integrating by parts autocorrelation for pressure and Fourier transform, integration, assumptions..

$$S(\mathbf{x},\omega) = \frac{\sqrt{\pi}}{16\pi^2\rho_0 c_0^5 x^2}\iiint \frac{\hat{q}_s^2}{c^2\tau_s} l_s^3\omega^2 \frac{e^{-\frac{\omega^2 l_s^2}{4\bar{u}^2}}}{1+\omega^2\tau_s^2} d\mathbf{x}_2$$

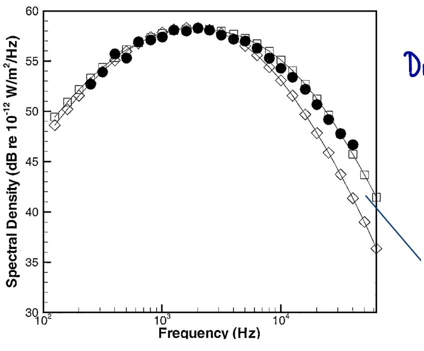

Different coefficient

Aircraft Noise Modelling

Categories

Transport Category and Jet Airplanes — Main source:
- HLD
- FAN
- LG
- JET

Helicopters — Main source:
- Engine
- Rotor
- Tail rotor
- Blade vortex interaction

Propeller Driven — Main source:
- Flap side-edge noise
- Propeller noise
- Wing slipstream interaction
- LG

Tiltrotors — Main source:
- Rotor noise

Noise prediction methods at system level

Full empirical methods: based on flight test data or component noise

Semi-empirical methods: based on measurements, recalibrated using analytical scaling laws.

Numerical methods: solution of flow governing equations

- Linearized Euler (LEE), potential equations (inviscid) ...
- URANS (viscous & Turbulence-modeled) → Aeroacoustics (engine tonal noise)
- LES, DES, LBM-VLES (viscous & turbulent)

Method vs application

Jet noise

Isolated, single-stream

- Semi-empirical methods: fast and sufficiently reliable.
  - Preliminary design, define an equivalent single stream jet in case of dual
  - Difficult to account for flight effects

Installed, realistic dual nozzles

Steady RANS
- Require tuning and robustness is weak
- Difficult to handle the effect of sheared flow on near field propagation.
- Interesting solution for preliminary design of realistic engines.

LES/DES/LBM-VLES most reliable solution, after careful validation looking at
- Mesh resolution, in the shear in particular.
- Dimension and location of the FW-H integration surface.
- Simulated physical time and dimension of the FW-H

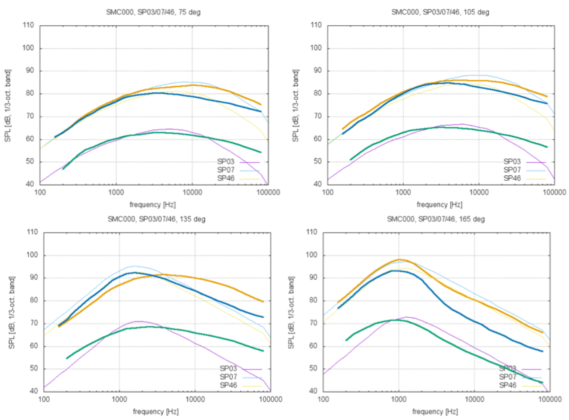

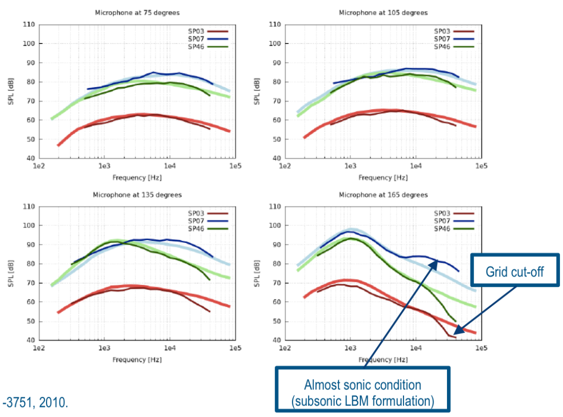

-3751, 2010.

FAN NOISE

- Axi-symmetric geometries:
  - Unsteady RANS (tonal) + semi empirical method (broadband)
    - Preliminary design, but they are sensitive to some parameters (not reliable)
    - Long and fragile chain, one method for one source mechanism.
    - Accurate tonal noise required turbulence-resolved formulations.
- Realistic engines:
  - LBM-VLES: only demonstrated reliable solution for tonal and broadband after checking:

    Mesh resolution, in particular around the rotor for correct wake simulation. (grey area problem)

    Dimension and location of the FW-H integration surface. (low attenuation, max pred. freq.)

    Simulated physical time for the min, predicted freq.

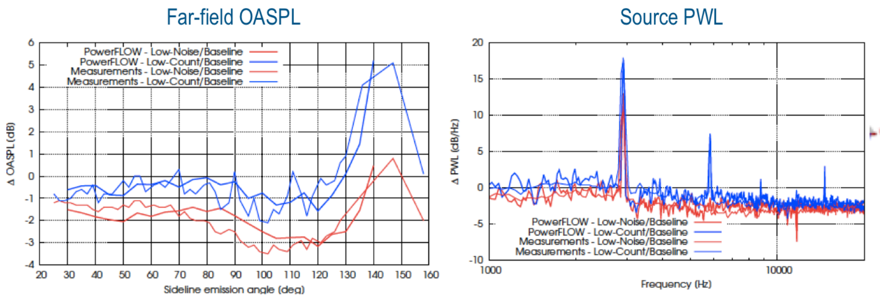

LANDING GEAR NOISE

Defeatured geometry

DES / LES: too expensive on final design

research scopes

difficult account for installation.

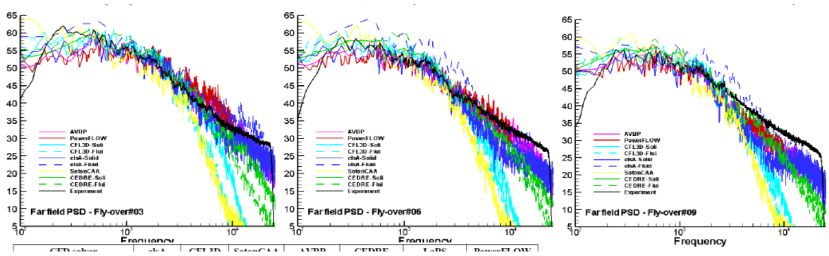

Realistic geometry

LBM-VLES: best between comp. cost, complexity and reliability. check for:

Fidelity on geometrical model (gaps, holes)

Dimensions and location of FW-H integration surface.

Simulated physical time and dimension of the FW-H for minimum predicted freq.

HLD Noise:

Defeatured geometry

DES / LES: too expensive on final design

research scopes

difficult account for installation.

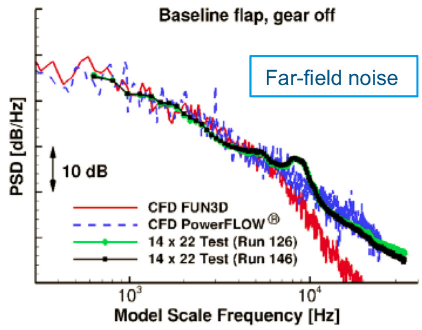

Realistic geometry

LBM-VLES: best between comp. cost, complexity and reliability. check for:

Fidelity on geometrical model (gaps, holes)

Simulated physical time and dimension of the FW-H for minimum predicted freq.

Rotor Propeller Noise

Tonnal noise, isolated:

Potential methods or blade element theory (loading noise)

- Not accurate and reliable in hover (wake)
- Limited to low speed

Steady RANS: best trade-off in design cycles.

Tonnal and/or bradband noise installed:

LBM-VLES: best tradeoff at system level.

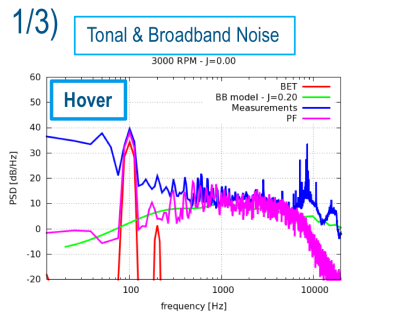

Blade Element Theory limited to tonal noise
Analytical broadband noise model not always reliable
Artefacts in the measurements (difficult to measure)
Simulations can be more reliable then experiments

Broadband Noise, isolated:

Potential methods + semi-analytical methods.

- Only trailing-edge noise and after calibration
- Not accurate and reliable in hover conditions
- Limited to low-speeds

LBM-VLES: best trade-off.

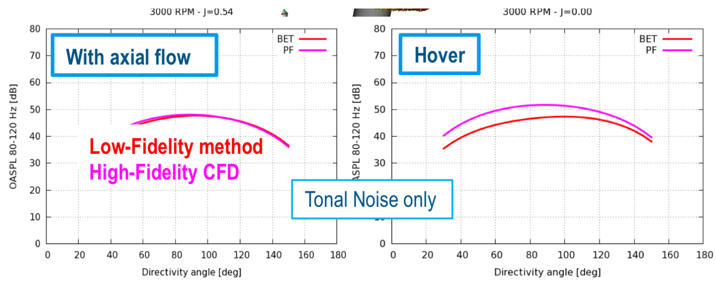

Helicopter BVI Noise

- Blade elastic deformation prescribed in the CFD model
  - URANS and LBM-VLES best trade-off on design.

Blade elastic deformation from a 2-way coupling with structural code

Potential method: only method used

- Determine elastic def for URANS and LBM-VLES

URANS: too expensive currently.

- Limited deterministic effects.

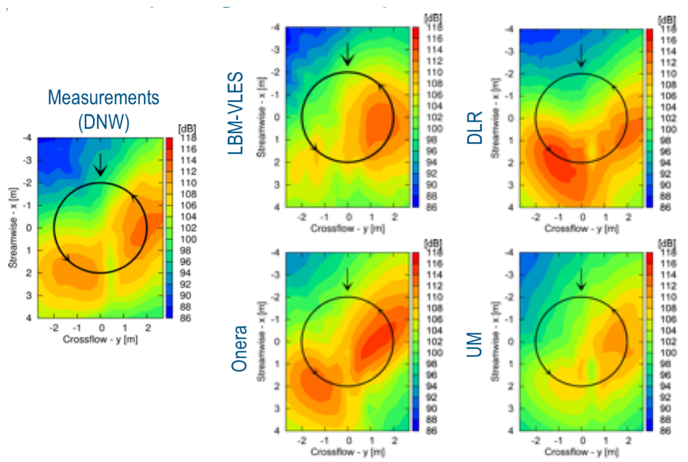

Noise Certification Procedure and Metric

14 CFR Part 36 – flight profiles – airplane/takeoff

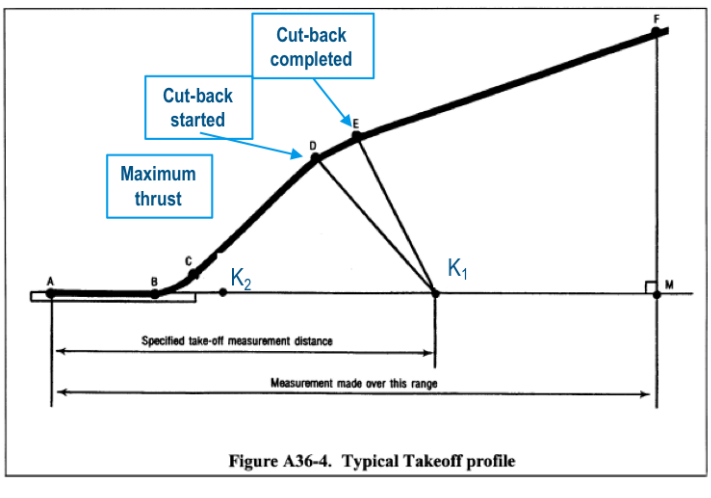

Figure A36-4. Typical Takeoff profile

(a) The airplane begins the takeoff roll at point A, lifts off at point B and begins its first climb at a constant angle at point C. Where thrust or power (as appropriate) cut-back is used, it is started at point D and completed at point E. From here, the airplane begins a second climb at a constant angle up to point F, the end of the noise certification takeoff flight path.

(b) Position K1 is the takeoff noise measuring station and AK1 is the distance from start of roll to the flyover measuring point. Position K2 is the lateral noise measuring station, which is located on a line parallel to, and the specified distance from, the runway center line where the noise level during takeoff is greatest.

(c) The distance AF is the distance over which the airplane position is measured and synchronized with the noise measurements, as required by section A36.2.3.2 of this part.

14 CFR Part 36 – flight profiles – airplane/approach

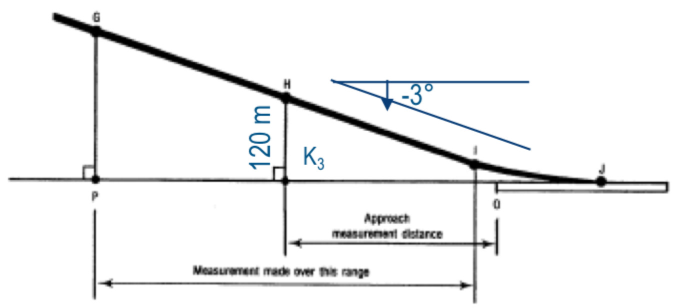

Figure A36-5. Typical Approach profile

(a) The airplane begins its noise certification approach flight path at point G and touches down on the runway at point J, at a distance OJ from the runway threshold.
(b) Position K3 is the approach noise measuring station and K3O is the distance from the approach noise measurement point to the runway threshold.
(c) The distance GI is the distance over which the airplane position is measured and synchronized with the noise measurements, as required by section A36.2.3.2 of this part.

14 CFR Part 36 – flight profiles – helicopter/takeoff

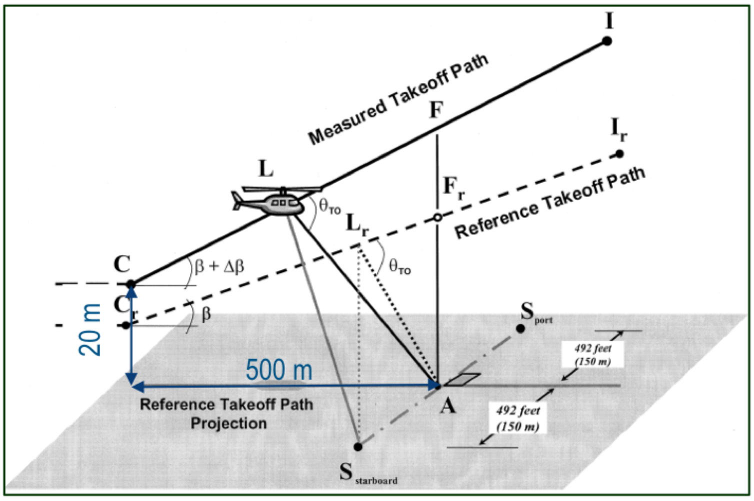

(2) The reference flight path is defined as a straight line segment inclined from the starting point C (1,640 feet (500 meters) from the center microphone location and 65 feet (20 meters) above ground level) at a constant climb angle β defined by the certificated best rate of climb and Vy for minimum engine performance. The constant climb angle β is derived from the manufacturer's data (approved by the FAA) to define the flight profile for the reference conditions. The constant climb angle β is drawn through Cr and continues, crossing over station A, to the position corresponding to the end of the type certification takeoff path represented by position Ir.

14 CFR Part 36 – flight profiles – helicopter/approach

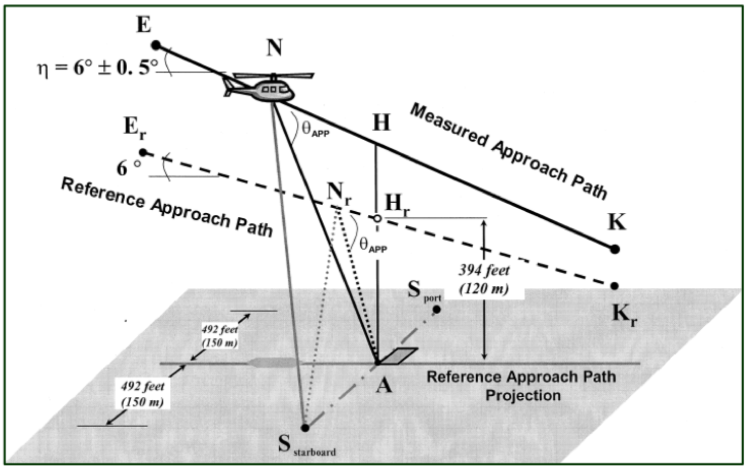

(i) The beginning of the approach profile is represented by helicopter position E. The position of the helicopter is recorded for a sufficient distance (EK) to ensure recording of the entire interval during which the measured helicopter noise level is within 10 dB of Maximum Tone Corrected Perceived Noise Level (PNLTM). The reference flight path, ErKr represents a stable flight condition in terms of torque, rpm, indicated airspeed, and rate of descent resulting in a 6° approach angle.
(ii) The test approach profile is defined by the approach angle η passing directly over the station A at a height of AH, to position K, which terminates the approach noise certification profile. The test approach angle η must be between 5.5° and 6.5°.
(2) The helicopter approaches position H along a constant 6° approach slope throughout the 10 dB down time period. The helicopter crosses position E and proceeds along the approach slope crossing over station A until it reaches position K.

14 CFR Part 36 – flight profiles – helicopter/fly-over

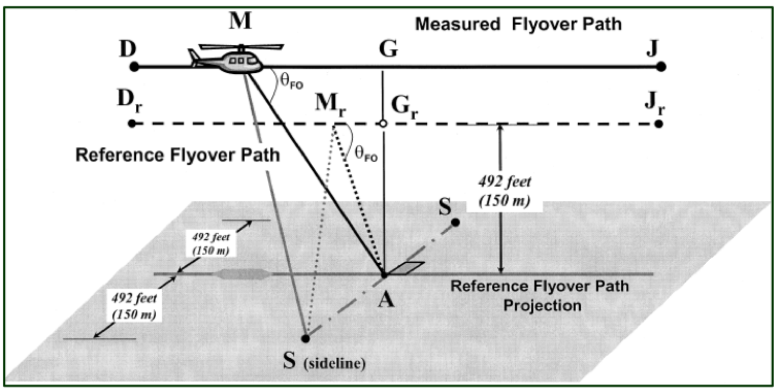

(d) Level flyover reference profile. The beginning of the level flyover reference profile is represented by helicopter position Dr (Figure H2). The helicopter approaches position Dr in level flight 492 feet above ground level as measured at Station A. Reference airspeed must be either 0.9VH; 0.9VNE; 0.45VH + 65 kts (0.45VH + 120km/h); or 0.45VNE + 65kts (0.45VNE + 120 km/h), whichever of the four speeds is least. The helicopter crosses directly overhead station A in level flight and proceeds to position Jr.

TEST CONDITIONS

Flat terrain

Not excesive sound absorption caracteristics

No precipitations

Air not above 35 °C not below -10 °C

Humidity not above 95 % not below 20%

Wind velocity : less than 12 knots, crosswind less than 7 knots

METRIC

1) For each flight segment k of the flight event of duration 0.5 s, computation of 1/3th octave band SPL in the frequency range [50 Hz:10 kHz] (band 17-40)

2) The $SPL_{i,k}$ levels in dB are converted into perceived noisiness coefficients using the following relationship:

$$n_{i,k} = \begin{cases} 10^{M_c(\mathrm{SPL}_{i,k}-\mathrm{SPL}_c)} & \text{if} \quad \mathrm{SPL}_a \leq \mathrm{SPL}_{i,k} \\ 10^{M_b(\mathrm{SPL}_{i,k}-\mathrm{SPL}_b)} & \text{if} \quad \mathrm{SPL}_b \leq \mathrm{SPL}_{i,k} < \mathrm{SPL}_a \\ 10^{M_e(\mathrm{SPL}_{i,k}-\mathrm{SPL}_e)} & \text{if} \quad \mathrm{SPL}_e \leq \mathrm{SPL}_{i,k} < \mathrm{SPL}_b \\ 10^{M_d(\mathrm{SPL}_{i,k}-\mathrm{SPL}_d)} & \text{if} \quad \mathrm{SPL}_d \leq \mathrm{SPL}_{i,k} < \mathrm{SPL}_c \end{cases}$$

where the reference SPL and slopes M are defined in Table (10).

1/3 Oct.band-16	SPL_a	SPL_b	SPL_c	SPL_d	SPL_e	M_b	M_c	M_d	M_e
1	91.0	64	52	49	55	0.043478	0.030103	0.079520	0.058098
2	85.9	60	51	44	51	0.040570	0.030103	0.068160	0.058098
3	87.3	56	49	39	46	0.036831	0.030103	0.068160	0.052288
4	79.9	53	47	34	42	0.036831	0.030103	0.059640	0.047534
5	79.8	51	46	30	39	0.035336	0.030103	0.053013	0.043573
6	76.0	48	45	27	36	0.033333	0.030103	0.053013	0.043573
7	74.0	46	43	24	33	0.033333	0.030103	0.053013	0.040221
8	74.9	44	42	21	30	0.032051	0.030103	0.053013	0.037349
9	94.6	42	41	18	27	0.030675	0.030103	0.053013	0.034859
10	∞	40	40	16	25	0.030103	N.A.	0.053013	0.034859
11	∞	40	40	16	25	0.030103	N.A.	0.053013	0.034859
12	∞	40	40	16	25	0.030103	N.A.	0.053013	0.034859
13	∞	40	40	16	25	0.030103	N.A.	0.053013	0.034859
14	∞	40	40	16	25	0.030103	N.A.	0.053013	0.034859
15	∞	38	38	15	23	0.030103	N.A.	0.059640	0.034859
16	∞	34	34	12	21	0.029960	N.A.	0.053013	0.040221
17	∞	32	32	9	18	0.029960	N.A.	0.053013	0.037349
18	∞	30	30	5	15	0.029960	N.A.	0.047712	0.034859
19	∞	29	29	4	14	0.029960	N.A.	0.047712	0.034859
20	∞	29	29	5	14	0.029960	N.A.	0.053013	0.034859
21	∞	30	30	6	15	0.029960	N.A.	0.053013	0.034859
22	∞	31	31	10	17	0.029960	N.A.	0.068160	0.037349
23	44.3	37	34	17	23	0.042285	0.029960	0.079520	0.037349
24	50.7	41	37	21	29	0.042285	0.029960	0.059640	0.043573

3) Then the noisiness of each band i is summed up to give the total perceived noisiness level N_k for the segment k , defined through:

$$N_k = 0.85 \max_{1}^{24}(n_{i,k}) + 0.15 \sum_{1}^{24} n_{i,k}$$

4) Then PNL is computed: $\mathrm{PNL}_k = 40 + \dfrac{10}{\log_{10}(2)} \log_{10}(N_k)$

5) An extra penalty needs to be incorporated into the total noise correction to take into account the annoyance of discrete tones that affect the human more negatively. The tone correction factors $c_{i,k}$ for each flight segment and for each bands are a computed on the base of the difference between actual and smoothed SPLs. The overall correction factor for the flight segment k is defined as: $C_k = \max_{1}^{24}(c_{i,k})$

6) The tone corrected PNL is then computed using the following formula:

$$\mathrm{PNLT}_k = \mathrm{PNL}_k + C_k$$

7) The final step of the procedure consists in integrating the PNLT curve in the time range [t_1 : t_2] where t_1 corresponds to the first time the PNLT is above the threshold $PNLT_{max}$ - 10 dB and t_2 correspond to the last recorded segment above the same threshold.

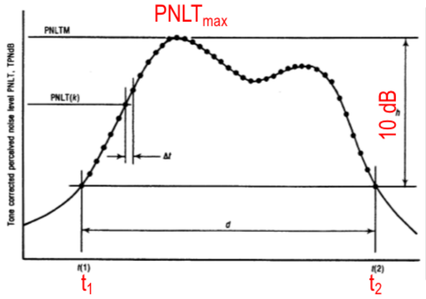

8) The EPNL is finally given by the following formula:

$$\mathrm{EPNL} = 10\log_{10}\left(\frac{1}{10\,\mathrm{s}}\int_{t_1}^{t_2} 10^{\frac{PNLT(t)}{10}}\,\mathrm{dt}\right)$$

EFFECT ON NOISE RESOLUTION